European Journal of Medicinal Chemistry 242 (2022) 114678

Contents lists available at ScienceDirect

European Journal of Medicinal Chemistry

journal homepage: www.elsevier.com/locate/ejmech

Synthesis and evaluation of novel furanones as biofilm inhibitors in opportunistic human pathogens

Andromeda-Celeste Gómez [a,b,1], Thérèse Lyons [c,1], Uwe Mamat [d,1], Daniel Yero [a,b], Marc Bravo [a,b], Xavier Daura [a,e,f], Osama Elshafee [g], Sascha Brunke [g], Cormac G.M. Gahan [c,h,i], Michelle O'Driscoll [c,j,k], Isidre Gibert [a,b,**], Timothy P. O'Sullivan [c,j,k,*]

[a] Institut de Biotecnologia i de Biomedicina, Universitat Autònoma de Barcelona, Barcelona, Spain
[b] Departament de Genètica i de Microbiologia, Universitat Autònoma de Barcelona, Barcelona, Spain
[c] School of Pharmacy, University College Cork, Cork, Ireland
[d] Cellular Microbiology, Research Center Borstel, Leibniz Lung Center, Parkallee 4a, 23845 Borstel, Germany
[e] Catalan Institution for Research and Advanced Studies (ICREA), Barcelona, Spain
[f] Biomedical Research Networking Center in Bioengineering, Biomaterials and Nanomedicine (CIBER-BBN), Barcelona, Spain
[g] Department of Microbial Pathogenicity Mechanisms, Leibniz Institute for Natural Product Research and Infection Biology – Hans Knoell Institute, Jena, Germany
[h] School of Microbiology, University College Cork, Cork, Ireland
[i] APC Microbiome Ireland, University College Cork, Cork, Ireland
[j] School of Chemistry, University College Cork, Cork, Ireland
[k] Analytical and Biological Chemistry Research Facility, University College Cork, Cork, Ireland

ARTICLE INFO

Keywords:
Furanones
Biofilms
Quorum sensing
Salmonella enterica
Staphylococcus aureus
Pseudomonas aeruginosa
Escherichia coli
Stenotrophomonas maltophilia
Candida albicans

ABSTRACT

Diseases caused by biofilm-forming pathogens are becoming increasingly prevalent and represent a major threat to human health. This trend has prompted a search for novel inhibitors of microbial biofilms which could, for example, be used to potentiate existing antibiotics. Naturally-occurring, halogenated furanones isolated from marine algae have proven to be effective biofilm inhibitors in several bacterial species. In this work, we report the synthesis of a library of novel furanones and their subsequent evaluation as biofilm inhibitors in several opportunistic human pathogens including *S. enterica*, *S. aureus*, *E. coli*, *S. maltophilia*, *P. aeruginosa* and *C. albicans*. A number of the most potent compounds were subjected to further analysis by confocal laser-scanning microscopy for their effects on *P. aeruginosa* and *C. albicans* biofilms individually, in addition to mixed polymicrobial biofilms. Lastly, we investigated the impact of a promising candidate on survival rates *in vivo* using a *Galleria mellonella* model.

1. Introduction

The discovery and development of antibiotics represents one of the major advances in human health [1,2]. Bacterial infections, which were previously potentially fatal, were suddenly made readily treatable [3,4]. However, even at the very early stages of the so-called 'golden age' of antibiotics, some warning signs were noted. In 1947, the first bacterial strain resistant to penicillin was identified and within a year of its clinical introduction, resistant strains of *Staphylococci* were isolated in patient samples [5].

As the use, overuse and misuse of antibiotics has increased over the intervening decades, so too has the problem of antimicrobial resistance (AMR). The World Bank has calculated that AMR could lead to ten million deaths each year by 2050, accompanied by an economic impact comparable to the 2008 financial collapse [6]. Over the next 35 years, 300 million are predicted to die prematurely as a result of AMR [7]. The six leading pathogens for deaths associated with resistance are *Escherichia coli*, *Staphylococcus aureus*, *Klebsiella pneumoniae*, *Streptococcus pneumoniae*, *Acinetobacter baumannii*, and *Pseudomonas aeruginosa*, in that order [8]. They constitute important opportunistic pathogens and are a frequent cause of nosocomial infections.

This challenge has been made all the greater by problems with the antibiotics pipeline where few new classes of antimicrobials have come

* Corresponding author. School of Pharmacy, University College Cork, Cork, Ireland.
** Corresponding author. Institut de Biotecnologia i de Biomedicina, Universitat Autònoma de Barcelona, Barcelona, Spain.
E-mail addresses: Isidre.Gibert@uab.cat (I. Gibert), tim.osullivan@ucc.ie (T.P. O'Sullivan).
[1] These authors contributed equally.

https://doi.org/10.1016/j.ejmech.2022.114678
Received 7 May 2022; Received in revised form 8 August 2022; Accepted 10 August 2022
Available online 20 August 2022

Abbreviations

AHL	Acyl Homoserine Lactone
AI-2	Autoinducer-2
AMR	Antimicrobial Resistance
CAL	*C. albicans* M2396
CLSM	Confocal laser-scanning microscopy
DME	Dimethoxyethane
DMSO	Dimethyl sulfoxide
ECO	*E. coli* ATCC 9637
LB	Lysogeny broth
NOESY	Nuclear Overhauser Effect Spectroscopy
PAO	*P. aeruginosa* PAO1
PAR	*P. aeruginosa* PAR7244
PBS	Phosphate-buffered saline
PCR	Polymerase chain reaction
QS	Quorum sensing
RFP	Red fluorescence protein
RBF	Round bottomed flask
SAU	*S. aureus* Newman
SEN	*S. enterica* sv. Typhimurium
SMA	*S. maltophilia* K279a
SOB	Super Optimal Broth
SPhos	2-Dicyclohexylphosphino-2′,6′-dimethoxybiphenyl
TSB	Tryptic Soy Broth
YPD	Yeast Extract–Peptone–Dextrose

to market in recent years. Only three new classes of antibiotics have been launched since 1990, and for one of these, the oxazolidiones, resistance was identified soon after their introduction [9].

Taking these factors into account, it is clear that new strategies are required. One such strategy involves targetting the resistance mechanisms of pathogenic bacteria, such as the production of biofilms. Biofilm-producing bacteria can be over 1000-fold more resistant to antimicrobials than their planktonic equivalents [10]. Additionally, the US National Institute of Health has noted that 80% of persistent infections in patients are associated with bacterial biofilms [11]. As biofilms are often polymicrobial in nature, the innate resistance of one population can reduce the susceptibility of another population in the biofilm leading to "herd-protection" [12]. Such polymicrobial infections are closely associated with diseases such as cystic fibrosis, ear and urinary infections, respiratory tract infections, diabetic ulcers, wounds, as well as with certain medical devices [13].

Biofilms are regulated by quorum sensing (QS), an intercellular communication system, which influences microbial virulence, secondary metabolites production and DNA uptake [14,15]. QS is coordinated by small signalling molecules known as autoinducers (AI). Autoinducers are biosynthesised by bacteria until their extracellular concentration reaches a particular threshold, which then triggers a change in gene expression [16]. One of the main autoinducers in Gram-negative bacteria are the *N*-acylated-L-homoserine lactones (AHLs). Autoinducer-2 (AI-2) is an intra- and interspecies communication molecule which has been identified in both Gram-negative and -positive bacteria. The development of new antimicrobial agents that interfere with bacterial quorum sensing, thereby inhibiting biofilm formation and increasing antibiotic sensitivity, has been the focus of significant research [17].

De Nys et al. have previously reported the isolation of halogenated furanones from the marine alga *Delisea pulchra* [18]. A number of these molecules were subsequently found to inhibit colonisation of the algal surface and were identified as potential anti-fouling agents, with bromofuranone **1** being recognised as one of the more promising candidates (Fig. 1) [19]. This discovery prompted further research into this class of compounds in the intervening years. A large number of halogenated furanones, and related synthetic analogues, were later discovered to inhibit biofilm formation in a variety of bacterial pathogens including *Salmonella enterica* sv. Typhimurium [20], *P. aeruginosa* [21], *E. coli* [22] and *Staphylococcus epidermis* [23]. We have previously reviewed the structure-activity relationships of these bioactive furanones, although the impact of structure on activity does vary considerably depending on the microbe under investigation [24]. It has been suggested that these compounds may constitute potential QS inhibitors. There is strong evidence that halogenated furanones, such as **2** and **3**, interfere with the AI-2 (**4**) signalling system present in several species [16,25]. For example, Zang et al. demonstrated that certain furanones deactivate the LuxS enzyme which plays a key role in the production of AI-2 [26]. Some evidence also exists that these compounds can inhibit AHL-dependent phenotypes [27,28].

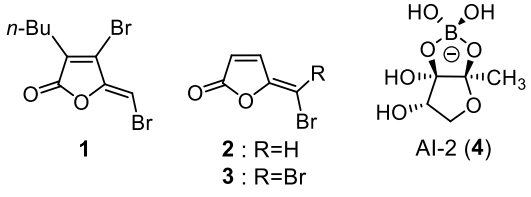

Fig. 1. Comparison of AI-2 with furanone-based quorum sensing inhibitors.

Herein, we describe the synthesis of a range of structurally diverse furanones using a variety of palladium-catayzed coupling reactions. These compounds are evaluated for their inhibitory effects on biofilm production in opportunistic human pathogens such as *S. enterica*, *S. aureus*, *P. aeruginosa*, *E. coli* and *S. maltophilia*, as well as the fungal pathogen *C. albicans*. The impact of furanone structure on biological activity is also discussed.

2. Results and Discussion

2.1. Chemistry

We have previously described the preparation of *gem*-dibromofuranone **3** from maleic anhydride *via* a modified Ramirez olefination [29]. Subsequent palladium-mediated coupling of **3**, in the presence of the SPhos ligand, was attempted with a variety of boronic acids (Table 1). In general, monoarylated furanones resulted when 1.1 equivalents of the boronic acid were employed and the reaction conducted at room temperature (entries 1, 4, 6, 8, 10). These couplings proceeded with high stereoselectivity, with formation of the *Z*-isomers favoured. Similar selectivity has been previously noted with comparable *gem*-dibromoolefin substrates [30–32]. The preparation of diarylated furanones was achieved by increasing the equivalents of boronic acid from 1.1 to 3, and by raising the reaction temperature to 100 °C (entries 2, 5, 7, 9, 11, 15). The introduction of a *m*- or *p*-nitro group to the arylboronic acid was associated with significantly reduced reactivity, and couplings failed to proceed at room temperature. When these reactions were repeated at 100 °C, a mixture of mono- and diarylated furanones were recovered (entries 12, 13). Attempted coupling of *p*-hydroxyphenylboronic acid under these conditions was not achieved and protodeboronation instead afforded phenol as the major by-product. By adapting the conditions developed by Noteberg and colleagues [33], where $Pd(OAc)_2$/SPhos was replaced with $Pd(PPh_3)_2Cl_2$ and DME/ethanol used in place of toluene, bis(phenol)-substituted furanone **21** was produced in 58% yield under microwave irradiation (entry 14).

Dibromoolefination of methylsuccinic anhydride (**23**) afforded a mixture of regioisomeric products (Scheme 1). 4-Methyl-substituted *gem*-dibromofuranone **24** was isolated in 46% yield along with minor

Table 1
Synthesis of arylated furanones *via* Suzuki coupling.

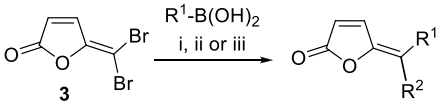

Entry	R^1	$R^1B(OH)_2$ (eq.)	Temp. (°C)	Conditions	Product	R^2	Yield
1		1.1	r.t.	i	**5**	Br	32%
2		3	100	ii	**6**		82%
3	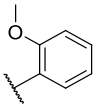	1.1	50	ii	**7**	Br	59%
					8	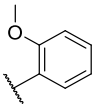	7%
4	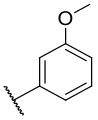	1.1	r.t.	i	**9**	Br	67%
5	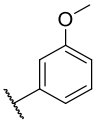	3	100	ii	**10**	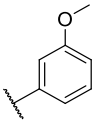	75%
6	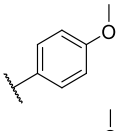	1.1	r.t.	i	**11**	Br	29%
7	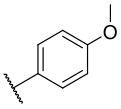	3	100	ii	**12**	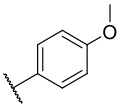	83%
8	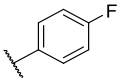	1	r.t.	i	**13**	Br	15%
9	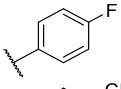	3	100	ii	**14**	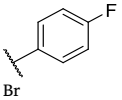	86%
10	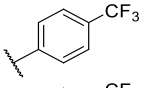	1	10	i	**15**	Br	26%
11	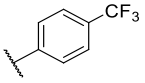	3	100	ii	**16**	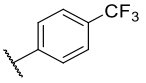	84%
12	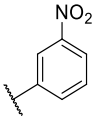	3	100	ii	**17**	Br	24%
					18	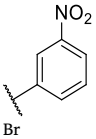	11%
13	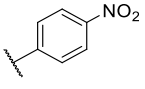	3	100	ii	**19**	Br	20%
					20	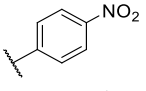	8%

(*continued on next page*)

Table 1 (*continued*)

14	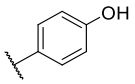	3	120	iii	**21**	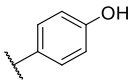	58%
15		3	100	ii	**22**		25%

i. $Pd(OAc)_2$ (3 mol%), SPhos (2 mol%), K_3PO_4 (2 eq.), PhMe, 48 h; ii. $Pd(OAc)_2$ (1 mol%), SPhos (2 mol%), K_3PO_4 (3 eq.), PhMe, 3 h; iii. $Pd(PPh_3)_2Cl_2$ (8 mol%), Na_2CO_3 (3 eq.), m.w., DME/EtOH 4:1, 40 min.

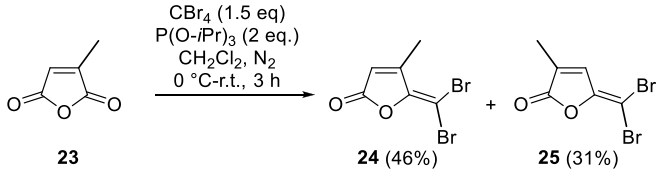

Scheme 1. Preparation of methylated *gem*-dibromofuranone 24.

product **25** in 31% yield. **25** has been previously investigated as a QS inhibitor and was not evaluated in this study [22].

The addition of an allylic halide to a furanone ring has been linked to improved QS activity [20,22,34]. With that in mind, a modified Ramirez olefination of anhydride **26**, prepared using a procedure described by Reynauld et al. [35], was attempted (Scheme 2). Treating **26** with a combination of carbon tetrabromide and triisopropyl phosphite furnished dibromoolefin **27** in 36% yield as the major product. Known furanone **28** was also identified as a minor product but proved impossible to isolate as a pure compound. **27** could be distinguished from regioisomer **28** by comparison of the chemical shift of H-3 at 6.58 ppm in **27** which was significantly upfield of the equivalent signal in **28** [35].

Several groups have investigated ring-brominated furanones as potential QS inhibitors [20,22,23,34,36]. Accordingly, a number of diarylated furanones were initially treated with bromine at reflux, followed by addition of triethylamine at 0 °C, to produce the corresponding ring-brominated furanones in high overall yields (Table 2). Bromination was found to proceed with high regioselectivity (entries 1–3), with the halogen introduced into the 3-position exclusively as confirmed by correlations between H-4 and the aromatic protons in 2D-NOESY spectra. The electron-donating effect of a 4-methoxy group led to the formation of two products, with concomitant *ortho*-bromination of the activated aromatic rings being observed (entry 2). Bromination of 4-trifluoromethylphenyl-substituted furanones in diethyl ether proceeded sluggishly with significant amounts of unreacted substrate recovered. Gratifyingly, switching to higher boiling point chloroform saw complete consumption of starting materials with a yield of 76% recorded (entry 3).

Chlorine- and iodine-containing furanones have received far less attention to date than their brominated analogues [24]. For example, *gem*-dichlorofuranone **33**, prepared by addition of trichloroacetate to succinic anhydride at reflux and subsequent acidification with concentrated sulfuric acid [37,38], has never been investigated for its QS activity (Scheme 3). A subsequent microwave-mediated Finkelstein reaction transformed **33** into *gem*-chloroiodofuranone **34** in 43% yield. Alternatively, Suzuki coupling of **33** with phenyl boronic acid furnished **35** solely as the *Z*-isomer in 50% yield. Coupling with 4-methoxyphenyl

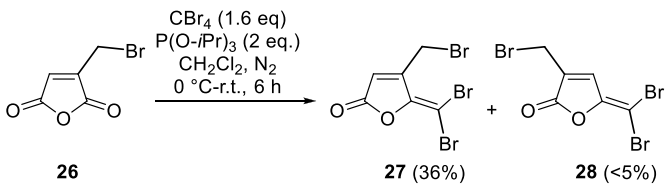

Scheme 2. Preparation of allylic bromide 27.

Table 2
Introduction of bromine onto the furanone ring.

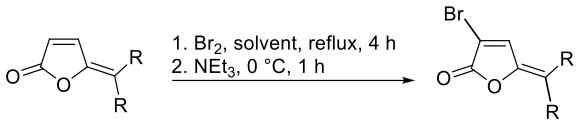

Entry	R	Solvent	Product	Yield
1		**Et_2O**	**29**	81%
2	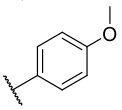	**Et_2O**	**30**	36%
	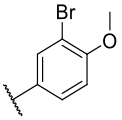	**Et_2O**	**31**	34%
3	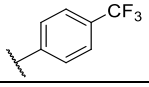	**$CHCl_3$**	**32**	76%

boronic acid proceeded more readily, with **36** recovered in 76% yield again as its *Z*-isomer. *gem*-Dichlorofuranone **34** proved to be a less reactive substrate than *gem*-dibromofuranone **3**, as reflected by the complete absence of diarylated equivalents of **35** or **36** after 48 h.

Furanones bearing alkyne substituents have exhibited promising QS inhibition against *P. aeruginosa* [36]. Sonogashira coupling of dibromoolefin **3** with 2.2 equivalents of 4-ethynylanisole at 80 °C furnished **37** exclusively in 34% yield under solvent-free conditions (Scheme 4). Attempted isolation of the corresponding monoalkynyl-substituted analogue using 1.1 equivalents of 4-ethynylanisole was ultimately unsuccessful, as the product was found to co-elute with trace amounts of **37**.

2.2. Biofilm inhibition activity of furanone library

Our library of novel furanones was next evaluated for their effects on different microorganisms of public health significance. We first tested their impact on microbial growth. Most of the compounds assessed did not impair growth significantly (Fig. 2). The largest effects were observed in the fungal pathogen *C. albicans*, with control furanones **2** and **3** inhibiting growth to the greatest extent. By contrast, both strains of *P. aeruginosa* proved largely insensitive to our library. These findings are of interest, as an ideal QS disruptor should minimally impact microbial growth, thus avoiding increased evolutionary pressure on the target.

S. enterica is a foodborne bacterium that colonises the gastrointestinal tract of infected individuals [39]. Tribromofuranone **27**, which incorporates an allylic bromide in addition to the common dibromoolefin motif, was the most active compound and significantly reduced

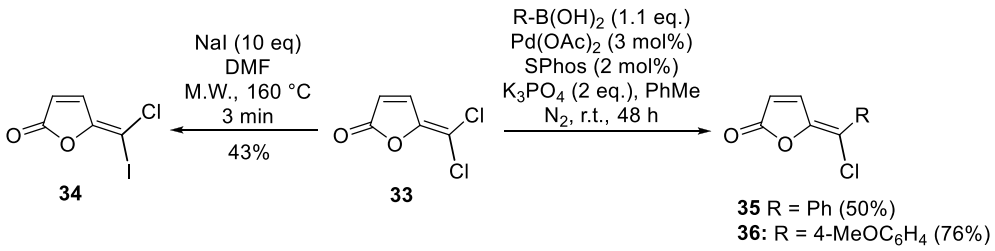

Scheme 3. Synthesis of chlorine- and iodine-containing furanones.

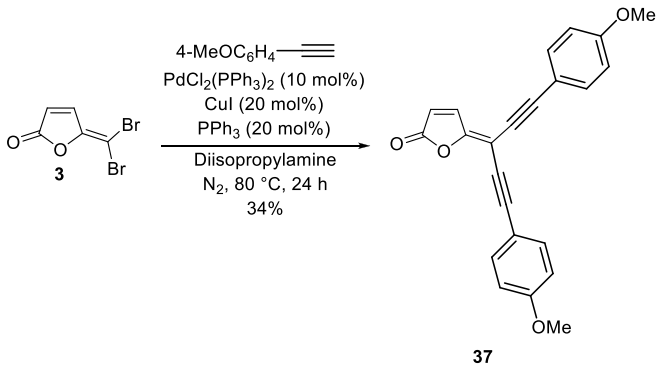

Scheme 4. Synthesis of 37 *via* Sonogashira coupling.

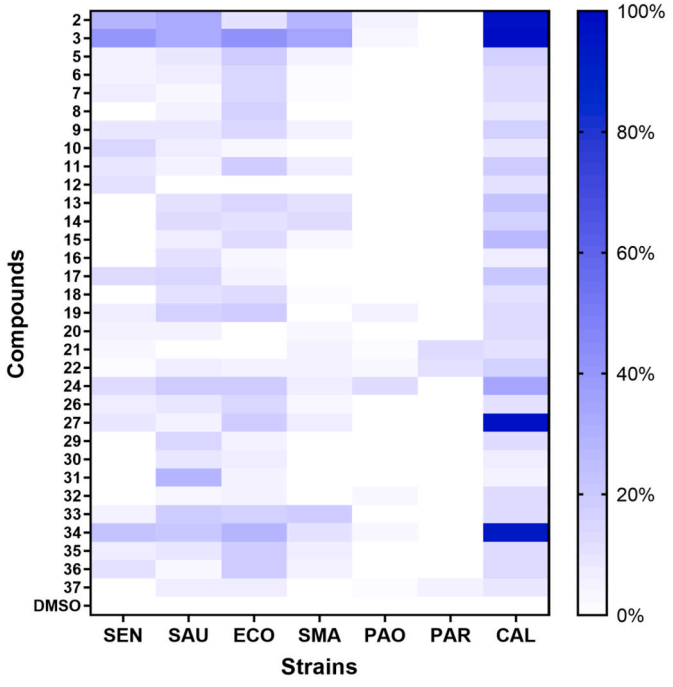

Fig. 2. Percentage growth inhibition by individual furanones. Heat map of mean growth inhibition values from at least three independent experiments for *S. enterica* sv. Typhimurium (SEN), *S. aureus* Newman (SAU), *E. coli* ATCC 9637 (ECO), *S. maltophilia* K279a (SMA), *P. aeruginosa* PAO1 (PAO), *P. aeruginosa* PAR7244 (PAR) and *C. albicans* M2396 (CAL). The scale displays 0%–100% growth inhibition at 50 μM concentration of each furanone. Controls contain the same volume of neat DMSO.

biofilm formation in *S. enterica* sv. Typhimurium by 72% at 50 μM concentration (Fig. 3 & Supplementary Figure B1). Known *gem*-dibromofuranone **3**, which was used as a control in this study, displayed comparable activity with 67% inhibition. Chlorine-substituted

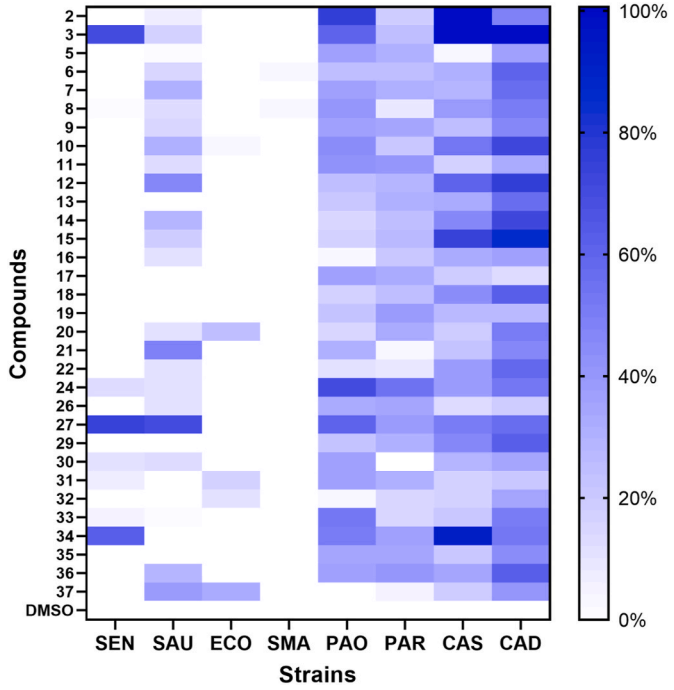

Fig. 3. Percentage biofilm inhibition by individual furanones. Heat map of mean biofilm inhibition values from at least three independent experiments for *S. enterica* sv. Typhimurium (SEN), *S. aureus* Newman (SAU), *E. coli* ATCC 9637 (ECO), *S. maltophilia* K279a (SMA), *P. aeruginosa* PAO1 (PAO), *P. aeruginosa* PAR7244 (PAR) and *C. albicans* M2396 (CA). For *C. albicans* M2396, inhibition of biofilm formation was analysed by sustained (CAS) and developmental (CAD) inhibition assays. The scale displays 0%–100% biofilm inhibition at 50 μM concentration of each furanone. Controls contained the same volume of neat DMSO.

furanones have traditionally been underexplored for their effects on bacterial biofilms. Interestingly, *gem*-chloroiodofuranone **34** was highly active with 59% inhibition recorded. Activity in *S. enterica* was quite structure specific, with most of our library having little or no impact on biofilm formation. Control **3** was found to reduce bacterial growth, along with **27** and **34** to a lesser extent (Fig. 2 & Supplementary Figure A1).

S. aureus is a Gram-positive opportunist bacterium that colonises the skin and mucosae of approximately 30% of the human population [40]. *S. aureus* causes a wide range of illnesses including impetigo, endocarditis, osteoarticular infection, pneumonia and toxic shock syndrome, as well as prosthetic device and catheter infections [41]. Methicillin-resistant *S. aureus* (MRSA) is currently responsible for 10 times more infections than all other multi-drug resistant Gram-negative pathogens combined [42]. MRSA poses a major challenge as current antimicrobial therapies are often associated with poor outcomes. As with *S. enterica*, tribromofuranone **27** was the most potent molecule, significantly inhibiting *S. aureus* Newman biofilm production by 71% (Fig. 3 & Supplementary Figure B2). Of the remaining candidates,

bis-4-hydroxyphenyl-substituted furanone **21** was the next most efficacious compound with 52% inhibition recorded. The structurally similar 4-methoxyphenyl-substituted analogue **12** displayed a comparable degree of inhibition, and reduced biofilm growth by 44%. Neither of these compounds contains a halogen atom, which is often considered a prequisite for biofilm-inihibiting furanones [24]. Transposing the methoxy group to either the 2- or 3-position saw a fall-off in activity with values of 7% recorded for **8** and 30% for **10**. 4-Methoxyphenylacetylene-substituted furanone **37**, a close analogue of **12** but incorporating an acetylene spacer, also exhibited a moderate effect (36% inhibition). Several of the biofilm inhibitors identified above (e.g. **12** and **21**) had minimal impact on bacterial growth (Supplementary Figure A2).

The Gram-negative bacterium *E. coli* is a common cause of several debilitating infections, including enteritis, urinary tract infections, septicaemia and neonatal meningitis [43]. The effect on biofilm production in *E. coli* ATCC 9637 was reduced relative to the other species under investigation (Fig. 3). Molecules lacking a dihaloolefin motif were generally more potent. Bis-4-methoxyphenylacetylene-substituted **37** was the most active compound, inhibiting biofilm growth by 31% (Supplementary Figure B3). The ring-brominated furanone **31** was moderately active with a 15% reduction noted. Neither of the two brominated controls **2** or **3** affected biofilm production. Several of these biofilm inhibitors moderately reduced bacterial growth in the order of 8% for **37** (Supplementary Figure A3). The largest effect was recorded with chloroiodofuranone **34** (28% reduction) which was not itself a biofilm inhibitor.

S. maltophilia is also an important nosocomial pathogen that has been linked to respiratory tract and blood infections, and is particularly significant in immunocompromised lung cancer patients [44]. None of our furanones inhibited growth (Supplementary Figure A4) or biofilm formation in *S. maltophilia* K279a (Fig. 3 & Supplementary Figure B4). The latter result is, perhaps, unsurprising as neither AI-2 nor AHL play significant roles in *S. maltophilia* QS [45].

P. aeruginosa is a significant driver of nosocomial infections, mainly in intensive unit care, where it is associated with ventilator-associated pneumonia, urinary tract infections, wound infections and various sepsis syndromes [46]. This pathogen poses a particular threat to immunocompromised patients [47]. In comparison to other bacteria, *P. aeruginosa* PAO1 biofilms proved sensitive to a wider range of furanone structures (Fig. 3). The most active compound was found to be control monobromofuranone **2** which inhibited biofilm growth by 75% (Supplementary Figure B5). Methyl-containing dibromofuranone **24** was almost equipotent with 70% inhibition observed. Its tribominated analogue **27**, which was the most active inhibitor of *S. enterica* and *S. aureus* biofilms, was slightly less effective against *P. aeruginosa* (60% inhibition). Although bromine-containing compounds were generally more potent, both dichlorofuranone **33** and chloroiodofuranone **34** inhibited biofilm production in *P. aeruginosa* PAO1 by 52% and 51% respectively. However, as with *S. enterica*, the presence of a halogen atom was not necessarily required for activity. Indeed, diarylated furanones **8** and **10**, which bear methoxy substituents at the 2- and 3-positions respectively, were found to be more active than their monoarylated equivalents **7** and **9**, and reduced biofilm growth by 41% and 44% respectively. None of the furanones inhibited the growth of *P. aeruginosa* PAO1 by more than 5% except for bromofuranone **24** which reduced bacterial growth by just 11% (Supplementary Figure A5). This is noteworthy as it suggests that these compounds reduce bacterial biofilm production without causing cell death, highlighting their potential as QS inhibitors.

P. aeruginosa PAR7244 is a recent clinical isolate identified in patients with tracheobronchitis and is classified as a high biofilm former [48]. In contrast to PAO1, biofilm production in PAR7244 was less sensitive overall (Fig. 3). Methyl-substituted dibromofuranone **24** was the most potent inhibitor, reducing biofilm growth significantly by 44% compared to a 70% reduction in PAO1 (Supplementary Figure B6). Surprisingly, control bromofuranone **2**, which was the most effective inhibitor in PAO1, had no impact on biofilm formation in PAR7244. As with PAO1, bacterial growth in *P. aeruginosa* PAR7244 was mostly unaffected by our library (Supplementary Figure A6).

While *C. albicans* is prevalent in the gastrointestinal and genitourinary tracts of healthy individuals, it may become pathogenic when the host's microbiota or immunity are disrupted [49,50]. *C. albicans* biofilms can be 1000 times more resistant to antimicrobials than their planktonic equivalents [51]. The presence of biofilm increases resistance to both antifungal agents and the host's immune system. Such biofilms pose a significant clinical challenge as they frequently form on implanted medical devices such as pacemakers, catheters and prosthetic joints [52]. Although a small number of brominated furanones have been investigated as fungal growth inhibitors of *C. albicans* [53], their impact on *Candida* biofilm formation remains unexplored.

Several furanones as analysed by sustained inhibition assays disrupted biofilm formation in *C. albicans* M2396 (Fig. 3). At 50 μM concentration, controls **2** and **3** completely inhibited biofilm production, with a strong inhibitory effect (92% inhibition) also observed for chloroiodofuranone **34** (Supplementary Figure B7). There was a noticeable overlap between compounds that inhibited biofilm formation with those furanones that also retarded cell growth (Supplementary Figure A7). By contrast, the next most active candidate, namely 4-trifluoromethylphenyl-substituted **15**, reduced biofilm production by 75% but had a much smaller effect on cell growth. Tribromofuranone **27**, which was the most potent inhibitor in several bacterial species, was less active against *C. albicans* biofilm with an inhibition value of 51%. The replacement of the two bromines in **3** with chlorines saw a fall-off in activity for **33** (21% inhibition). Other structural changes, such as the introduction of a methyl group onto the C4-position of the furanone ring, were similarly detrimental with **24** reducing biofilm formation by only 38%. As previously observed with bacterial biofilms, the presence of a vinylic halogen was not a prequisite for activity. Bis-4-methoxyphenyl-substituted furanone **12** and the closely related bis-3-methoxyphenyl-substituted furanone **10** reduced fungal biofilm growth by 61% and 53% respectively.

We also examined the effect of our library on biofilm growth in the developmental phase of *C. albicans* M2396 where a different pattern emerged. In particular, the correlation of inhibitory effects on biofilm growth with cell growth was less pronounced. Once again, dibromofuranone **3** completely inhibited *Candida* biofilm, but monobromofuranone **2** proved much less effective (Supplementary Figure B8). 4-Trifluoromethylphenyl-substituted **15** was more active in the developmental phase with 85% inhibition recorded. Non-halogenated bis-4-methoxyphenyl-substituted furanone **12** and bis-3-methoxyphenyl-substituted furanone **10** reduced fungal biofilm growth by 75% and 71% respectively. A reduced inhibitory effect was observed with chloroiodofuranone **34** (52% inhibition) in the developmental phase.

2.3. Disruption of mixed bacterial-fungal biofilms by selected furanones

In both natural and clinical environments, biofilms are often polymicrobial in composition. Inter-kingdom (e.g. bacteria/fungi) biofilms, such *P. aeruginosa*/*C. albicans*, have been identified in infections of the lungs, skin and in medical devices [13]. When these microorganisms are co-isolated, their interaction may be simultaneously competitive, synergistic and/or antagonistic [54]. We wondered if our furanones with significant anti-biofilm activity were also capable of disrupting mixed fungal-bacterial biofilms. The chosen furanones were initially subjected to further analysis for their effect on single-species biofilms of *P. aeruginosa* and *C. albicans* using confocal laser-scanning microscopy (CLSM). Under these conditions, some of the compounds assayed disrupted biofilm formation in both target pathogens (Fig. 4). These results were in accordance with those obtained by the crystal violet staining method (Supplementary Figure B5) and the XTT reduction assay (Supplementary Figure B7) using microtiter plates. For *C. albicans*, the most

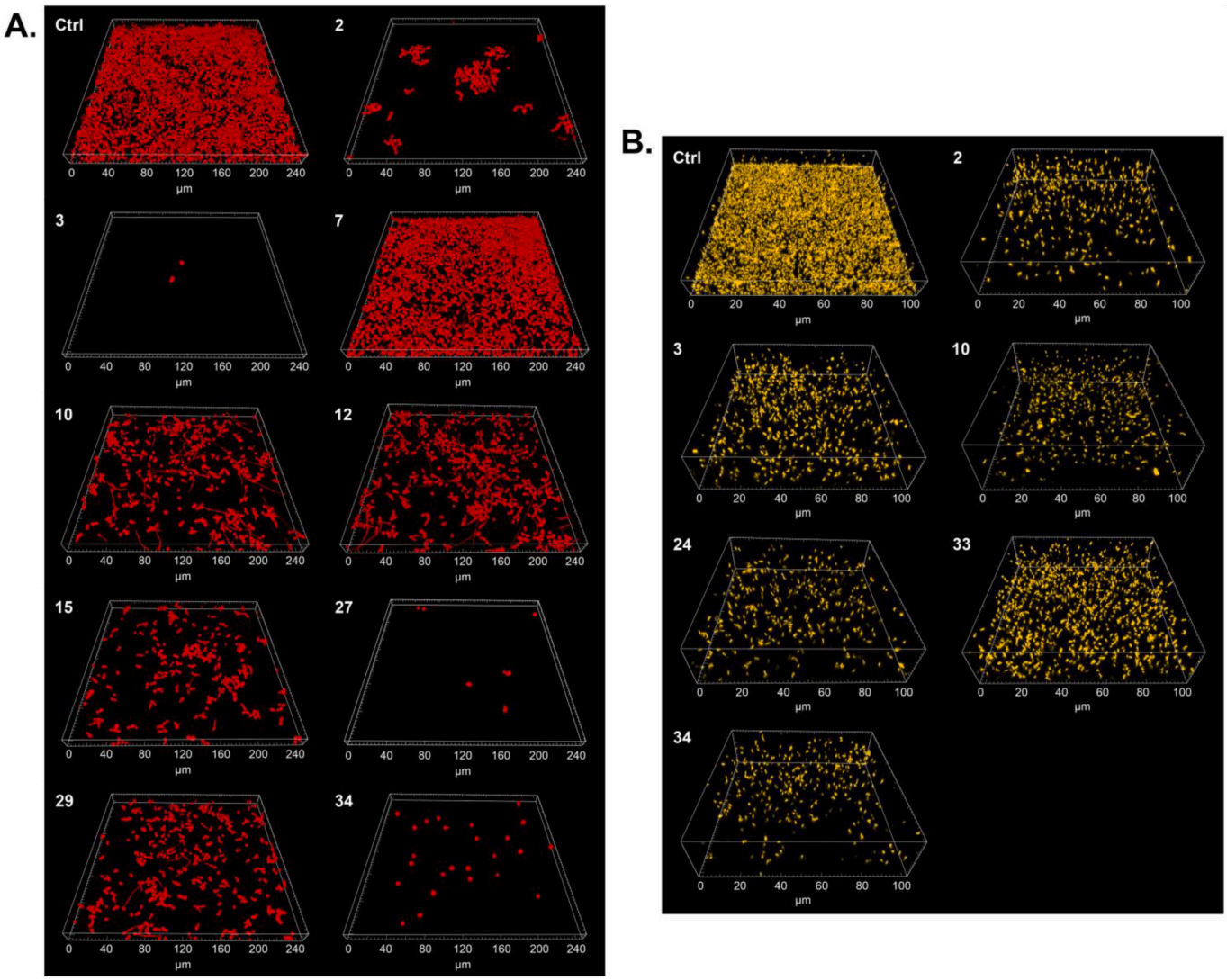

Fig. 4. Furanones with significant anti-biofilm activity as analysed by confocal laser-scanning microscopy (CLSM). (A) CLSM images of *C. albicans* M2396 in the presence of **2**, **3**, **7**, **10, 12, 15, 27, 29** and **34**. (B) Representative CLSM images of biofilm formed by *P. aeruginosa* PAO1 in the presence of **2**, **3**, **10**, **24**, **33** and **34**. In both panels, control (Ctrl) represents biofilms treated with neat DMSO.

pronounced effects were observed with bromofuranones **2**, **3**, tribromofuranone **27** and chloroiodofuranone **34** (Fig. 4A). Chloroiodofuranone **34** was also one of the most effective compounds against *P. aeruginosa* PAO1 (Fig. 4B).

Based on these results, we studied the effect of bromofuranones **2**, **3** and chloroiodofuranone **34** on the formation of mixed biofilms composed of both species. Fig. 5 shows CLSM images of dual-species biofilms formed by *C. albicans* M2396 with *P. aeruginosa* PAO1. Under the growth conditions used, *C. albicans* showed less adherence to μ-Slides than *P. aeruginosa*, probably due to the inhibitory effect of *P. aeruginosa* exoproducts on the fungus [13]. Bromofuranones **2**, **3** and chloroiodofuranone **34** were all found to decrease the biomass of both microorganisms within the mixed biofilms (Fig. 5).

2.4. *In vitro and in vivo toxicity and efficacy of candidate compounds*

We next evaluated the toxicity of our most promising furanones *in vitro* and *in vivo*, using HK-2 human kidney cells and *G. mellonella* larvae respectively. We first examined the *in vitro* effect of **2**, **10**, **24**, **27** and **33** at 50 μM on the HK-2 human cell line. Bis-3-methoxyphenyl-substituted furanone **10** showed no indication of significant toxicity (Fig. 6A). **10** was the sole non-halogenated furanone in this group which may account for its reduced toxicity. The other compounds tested, namely **2**, **24**, **27** and **33**, proved toxic to human kidney cells which could prevent their use in humans, at least in their current formulation (data not shown). By contrast, *in vivo* toxicity screening of the same compounds at double concentration (100 μM) showed that none was toxic to the larvae as no animal died or showed signs of melanization (Fig. 6B). Toxicity testing in *G. mellonella* larvae has recently emerged as a reliable predictor of chemical toxicity [55].

Since **10** was non-toxic in human cells, we investigated its *in vivo* antimicrobial activity in the *G. mellonella* acute model following infection with *P. aeruginosa*. The strain PAO1 is known to be highly virulent for *Galleria* larvae [56]. Despite the low concentration tested (100 cfu per larva), we recorded 100% mortality after 24 h (data not shown). We instead infected the larvae with the clinical isolate PAR7244 which has been shown to be less virulent for *Galleria* [48]. Treatment with **10** resulted in a significant increase in larvae survival (72%) compared with non-treated larvae at 48% survival (Fig. 7). Furanone **10** was not associated with significant biofilm inhibition in *P. aeruginosa* PAR7244 (Supplementary Figure B6), so the basis of increased larval survival remains to be elucidated.

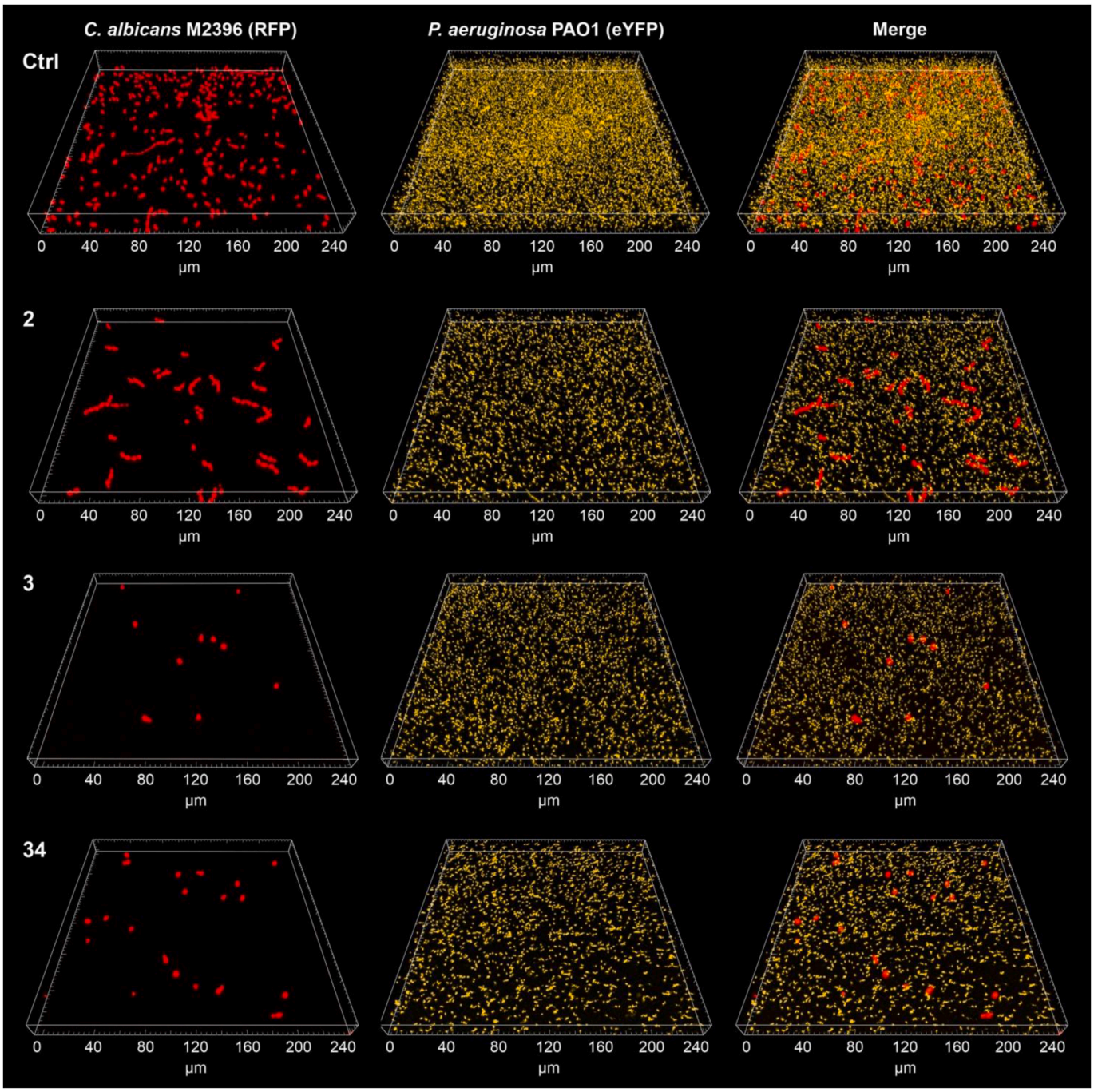

Fig. 5. Confocal laser-scaning microscopy (CLSM) images of dual-species biofilms formed by *C. albicans* M2396 (red) and *P. aeruginosa* PAO1 (yellow) in the presence of furnanones **2**, **3** and **34**. The control (Ctrl) represents a mixed biofilm treated with neat DMSO.

3. Conclusion

We have described the synthesis of a variety of bromine-, chlorine- and iodine-containing furanones which were subjected to further modification *via* Pd-catalysed coupling reactions. Several compounds in this diverse library were found to strongly inhibit bacterial biofilm formation in *S. enterica*, *S. aureus*, *P. aeruginosa* and to a lesser extent in *E. coli*. In particular, tribromofuranone **27** exhibited equal or better inhibitory activity against *S. enterica*, *S. aureus*, *P. aeruginosa* compared to known dibromofuranones **2** or **3**. Compounds which inhibited biofilm formation did not generally impact on bacterial growth, highlighting their potential as QS inhibitors. A number of compounds were also found to impede biofilm growth in the fungal pathogen *C. albicans* with 4-trifluoromethylphenyl-substituted **15** being identified as a promising candidate. These effects were confirmed by confocal laser-scaning microscopy. While compound cytotoxicity was identified as a potential issue, this was not replicated in toxicity testing with *G. mellonella*. Interestingly, diarylated furanone **10** was not only found to be non-toxic but also increased the survival rates of *G. mellonella* infected with *P. aeruginosa* PAR7244.

The discovery of antibiotics remains one of the crowning achievements of the 20th century. However, since their introduction, the problem of antimicrobial resistance has grown exponentially, with ever more cases of resistant infections being reported in the literature. Diseases caused by resistant bacteria now constitute the second most common cause of death globally [57]. It is clear that a multipronged

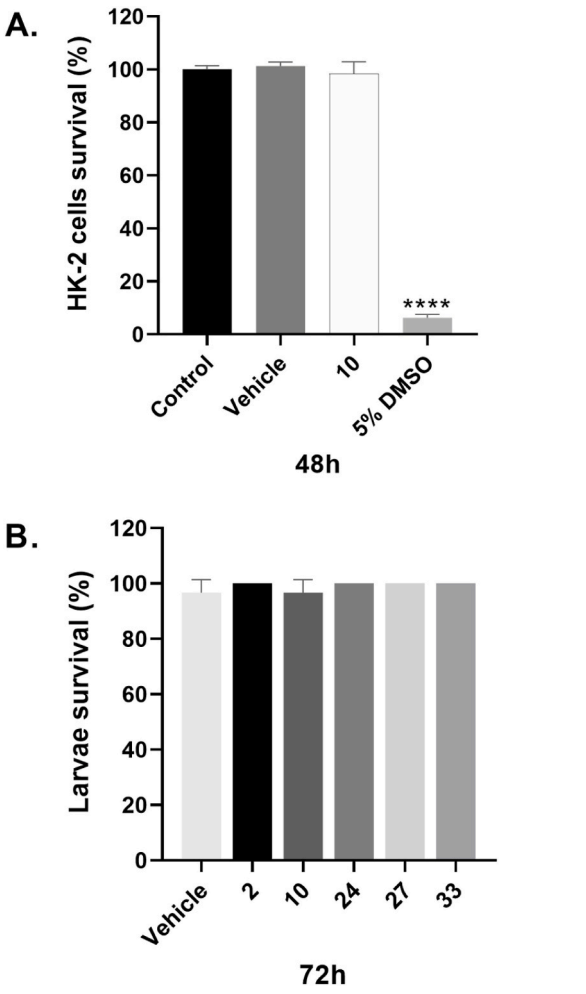

Fig. 6. *In vitro* and *in vivo* toxicity of selected furanones. A) Cytotoxicity in human kidney cells. MTT-based assay with furanone **10** at a concentration of 50 μM on HK-2 cells. The viability percentage was calculated using non-treated cells (Control). Vehicle is DMSO with a concentration of 0.5%. DMSO 5% was used as a cytotoxicity control. B) Toxicity in *G. mellonella* of **2**, **10**, **24**, **27** and **33** at 100 μM. Vehicle is DMSO with a concentration of 1%. The surviving percentage was calculated using larvae injected with the vehicle.

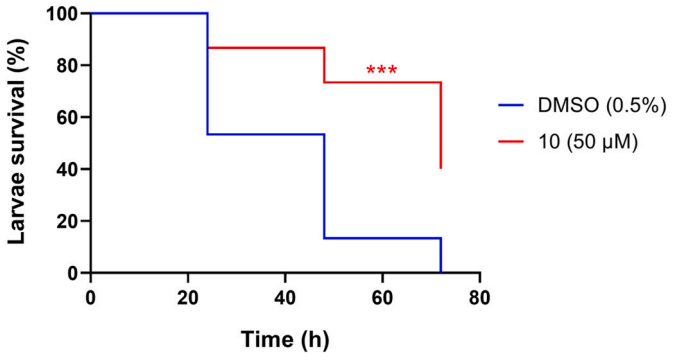

Fig. 7. Kaplan-Meier survival curves of *G. mellonella* larvae infected with *P. aeruginosa* PAR7244. The larvae were treated with furanone **10** at a concentration of 50 μM in PBS (difference significant by log-rank test, $P < 0.001$). DMSO at concentrations of 0.5% in PBS was used as vehicle control for untreated animals.

approach to tackling AMR is required. The use of small molecule inhibitors of QS has long been touted as one promising strategy. The results reported here support this approach for the treatment of common nocosomial infections.

4. Experimental section

4.1. Chemistry

Known compounds **2** [58], **3** [29,59] & **33** [29,37] were prepared *via* previously reported procedures. Analytical data are provided as Supplementary data.

4.1.1. General procedure for the preparation of monoarylated furanones

To an oven-dried RBF was added **3** (202 mg, 0.787 mmol, 1 eq.), the appropriate boronic acid (0.866 mmol, 1.1 eq.), tripotassium phosphate (334 mg, 1.574 mmol, 2 eq.), palladium(II) acetate (5 mg, 3 mol%), SPhos (7 mg, 2 mol%) and toluene (4 mL) under a flow of nitrogen. The reaction mixture was stirred at room temperature for 48 h and then diluted with dichloromethane (30 mL). The solution was filtered through a layer of Celite and the solvents were evaporated under reduced pressure. The crude product was purified *via* column chromatography with 4%–8% ethyl acetate in hexane to afford the monoarylated furanone product.

4.1.1.1. *(Z)-5-(Bromo(phenyl)methylene)furan-2(5H)-one (5) [32].* Yield: 32%

^{1}H NMR ($CDCl_3$, 400 MHz): 6.32 (1H, d, $J = 5.5$ Hz, **H**-3), 7.42–7.48 (6H, m, **H**-4, **H**-2′, **H**-3′, **H**-4′, **H**-5′, **H**-6′); ^{13}C NMR ($CDCl_3$, 100 MHz): 110.98 (**C**Br), 120.81 (**C**3), 128.78 and 130.12 (**C**2′, **C**6′, **C**3′, **C**5′), 130.27 (**C**4′), 135.36 (**C**1’), 140.96 (**C**4), 149.08 (**C**5), 168.53 (**C**2); IR (ATR, cm^{-1}): 2922, 1776, 1759, 1624, 1547, 1487, 1444, 1230, 1107, 1069, 1033, 955, 925, 902, 861, 809, 755, 711. 693, 627; HRMS (ESI^+): Exact mass calculated for $C_{11}H_8BrO_2^+$ $[M+H]^+ = 250.9708$; Found = 250.9704.

4.1.1.2. (Z)-5-(Bromo(2-methoxyphenyl)methylene)furan-2(5H)-one (7). Yield: 59%

^{1}H NMR ($CDCl_3$, 400 MHz): 3.86 (3H, s, O**CH$_3$**), 6.23 (1H, d, $J = 5.5$ Hz, **H**-3), 6.96–7.02 (2H, m, **H**-3′, **H**-5′), 7.17 (1H, d, $J = 5.5$ Hz **H**-4), 7.25–7.28 (1H, m, **H**-6′), 7.42 (1H, td, $J = 7.8$ Hz, 1.31 Hz, **H**-4′); ^{13}C NMR ($CDCl_3$, 100 MHz): 55.79 (O**C**H$_3$), 106.13 (**C**Br), 111.59 (**C**3′), 120.11 (**C**3), 120.57 (**C**5′), 123.63 (**C**1′), 131.87 (**C**4′), 132.03 (**C**6’), 141.11 (**C**4), 149.92 (**C**5), 157.47 (**C**OCH$_3$), 168.82 (**C**2); IR (ATR, cm^{-1}): 3071, 2932, 2839, 1776, 1762, 1595, 1578, 1488, 1462, 1250, 1108, 1068, 1048, 956, 862, 810, 776, 754, 704, 624,; HRMS (ESI^+): Exact mass calculated for $C_{12}H_{10}BrO_3^+$ $[M+H]^+ = 280.9813$; Found = 280.9806.

4.1.1.3. (Z)-5-(Bromo(3-methoxyphenyl)methylene)furan-2(5H)-one (9). Yield: 67%

^{1}H NMR ($CDCl_3$, 400 MHz): 3.85 (3H, s, O**CH$_3$**), 6.31 (1H, d, $J = 5.5$ Hz, **H**-3), 6.97–7.03 (3H, m, **H**-2′, **H**-4′, **H**-6′), 7.32 (1H, t, $J = 7.8$ Hz, **H**-5′), 7.46 (1H, d, $J = 5.5$ Hz, **H**-4); ^{13}C NMR ($CDCl_3$, 100 MHz): 55.48 (O**C**H$_3$), 110.65 (**C**Br), 115.72 (**C**2′), 115.88 (**C**4′), 120.75 (**C**3), 122.43 (**C**6′), 129.77 (**C**5′), 136.54 (**C**1′), 141.04 (**C**4), 149.15 (**C**5), 159.62 (**C**3’), 168.51 (**C**2); IR (ATR, cm^{-1}): 3139, 2937, 2843, 1782, 1758, 1596, 1576, 1548, 1486, 1427, 1287, 1251, 1202, 1108, 1049, 1033, 976, 883, 812, 774, 711, 690; HRMS (ESI^+): Exact mass calculated for $C_{12}H_{10}BrO_3^+$ $[M+H]^+ = 280.9813$; Found = 280.9806.

4.1.1.4. (Z)-5-(Bromo(4-methoxyphenyl)methylene)furan-2(5H)-one (11). Yield: 29%

^{1}H NMR ($CDCl_3$, 300 MHz): 3.86 (3H, s, O**CH$_3$**), 6.29 (1H, d, $J = 5.5$ Hz, **H**-3), 6.95 (2H, dt, $J = 8.9$ Hz, 3.0 Hz, **H**-3′, **H**-5′), 7.40–7.44 (3H, m,

H-4, **H**-2′, **H**-6′); ^{13}C NMR ($CDCl_3$, 75.5 MHz): 55.53 (O**C**H_3), 111.43 (**C**Br), 114.18 (**C**3′, **C**5′), 120.31 (**C**3), 127.64 (**C**1′), 131.63 (**C**2′, **C**6′), 140.91 (**C**4), 148.43 (**C**5), 161.19 (**C**4'), 168.71 (**C**2); IR (ATR, cm^{-1}): 3138, 3109, 2840, 1759, 1776, 1602, 1508, 1545, 1253, 1237, 1175, 1110, 1031, 904, 864, 809, 703, 579; HRMS (ESI^+): Exact mass calculated for $C_{12}H_{10}BrO_3^+$ $[M+H]^+$ = 280.9813; Found = 280.9803.

4.1.1.5. (Z)-5-(Bromo(4-fluorophenyl)methylene)furan-2(5H)-one (13). Yield: 15%

^{1}H NMR ($CDCl_3$, 400 MHz): 6.34 (1H, d, *J* = 5.5 Hz, **H**-3), 7.14 (2H, t, *J* = 8.6 Hz, **H**-3′, **H**-5′), 7.39 (1H, d, *J* = 5.5 Hz, **H**-4), 7.45–7.48 (2H, m, **H**-2′, **H**-6′); ^{13}C NMR ($CDCl_3$, 100 MHz): 109.55 (**C**Br), 116.02 (d, *J* = 22.2 Hz, **C**3′, **C**5′), 121.08 (**C**3), 131.47 (d, *J* = 3.4 Hz, **C**1′), 132.07 (d, *J* = 8.7 Hz, **C**2′, **C**6′), 140.58 (**C**4), 149.14 (**C**5), 163.65 (d, *J* = 252.2 Hz, **C**4'), 168.37 (**C**2); IR (ATR, cm^{-1}): 3072, 2955, 2853, 2922, 1782, 1765, 1601, 1549, 1505, 1236, 1106, 866, 807, 567, 535; HRMS (ESI^+): Exact mass calculated for $C_{11}H_7BrFO_2^+$ $[M+H]^+$ = 268.9613; Found = 268.9607.

4.1.1.6. (Z)-5-(Bromo(4-(trifluoromethyl)phenyl)methylene)furan-2(5H)-one (15). Yield: 26%

^{1}H NMR ($CDCl_3$, 400 MHz): 6.39 (1H, d, *J* = 5.5 Hz, **H**-3), 7.41 (1H, d, *J* = 5.5 Hz, **H**-4), 7.60 (2H, d, *J* = 8.1 Hz, **H**-2′, **H**-6′), 7.72 (2H, d, *J* = 8.1 Hz, **H**-3′, **H**-5′); ^{13}C NMR ($CDCl_3$, 75.5 MHz): 108.42 (**C**Br), 121.75 (**C**3), 123.37 (q, *J* = 272.5 Hz, **C**F_3), 125.81 (q, *J* = 3.8 Hz, **C**3′, **C**5′), 130.50 (**C**2′, **C**6′), 132.04 (q, *J* = 32.9 Hz, **C**4′), 138.87 (**C**1'), 140.35 (**C**4), 149.86 (**C**5), 168.01 (**C**2); IR (ATR, cm^{-1}): 2957, 2923, 2853, 1782, 1765, 1615, 1551, 1408, 1320, 1166, 1122, 1104, 1065, 1018, 957, 844, 809, 765, 710, 600,; HRMS (ESI^+): Exact mass calculated for $C_{12}H_7BrF_3O_2^+$ $[M+H]^+$ = 318.9582; Found = 318.9574.

4.1.1.7. (Z)-5-(Bromo(3-nitrophenyl)methylene)furan-2(5H)-one (17). Yield: 24%

^{1}H NMR ($CDCl_3$, 300 MHz): 6.43 (1H, d, *J* = 5.6 Hz, **H**-3), 7.41 (1H, d, *J* = 5.6 Hz, **H**-4), 7.67 (1H, td, *J* = 8.0 Hz, 0.64 Hz, **H**-5′), 7.82 (1H, ddd, *J* = 8.0 Hz, 1.6 Hz, 1.2 Hz, **H**-6′), 8.30–8.34 (2H, m, **H**-2′, **H**-4′); ^{13}C NMR ($CDCl_3$, 75.5 MHz): 106.88 (**C**Br), 122.30 (**C**3), 124.75 (**C**2′), 124.84 (**C**4′), 130.05 (**C**5′), 135.77 (**C**6′), 137.09 (**C**1′), 139.92 (**C**4), 148.31 (**C**5), 150.22 (**C**3'), 167.68 (**C**2); IR (ATR, cm^{-1}): 3081, 2904, 2854, 1781, 1762, 1612, 1550, 1528, 1474, 1348, 1290, 1107, 984, 882, 812, 737, 676; HRMS (ESI^+): Exact mass calculated for $C_{11}H_7BrNO_4^+$ $[M+H]^+$ = 295.9558; Found = 295.9551.

4.1.1.8. (Z)-5-(Bromo(4-nitrophenyl)methylene)furan-2(5H)-one (19). Yield: 20%

^{1}H NMR ($CDCl_3$, 400 MHz): 6.44 (1H, d, *J* = 5.6 Hz, **H**-3), 7.41 (1H, d, *J* = 5.6 Hz, **H**-4), 7.67 (2H, d, *J* = 8.7 Hz, **H**-2′, **H**-6′), 8.32 (2H, d, *J* = 8.7 Hz, **H**-3′, **H**-5′); ^{13}C NMR ($CDCl_3$, 100 MHz): 107.18 (**C**Br), 122.36 (**C**3), 123.99 (**C**3′, **C**5′), 131.10 (**C**2′, **C**6′), 140.02 (**C**4), 141.55 (**C**1′), 148.46 (**C**4'), 150.32 (**C**5), 167.67 (**C**2); IR (ATR, cm^{-1}): 3141, 3108, 3053, 1770, 1767, 1595, 1551, 1517, 1346, 1232, 1108, 1033, 957, 859, 767; HRMS (ESI^+): Exact mass calculated for $C_{11}H_7BrNO_4^+$ $[M+H]^+$ = 295.9558; Found = 295.9548.

4.1.2. General procedure for the preparation of diarylated furanones

To an oven-dried RBF was added **3** (200 mg, 0.787 mmol, 1 eq.), the appropriate boronic acid (2.361 mmol, 3 eq.), tripotassium phosphate (501 mg, 2.361 mmol, 3 eq.), palladium(II) acetate (3 mg, 1 mol%), SPhos (7 mg, 2 mol%) and toluene (5 mL). The reaction mixture was heated to 100 °C for 3 h under a flow of nitrogen. The reaction was cooled to room temperature and dichloromethane (30 mL) was added to the reaction flask. The solution was filtered through a layer of Celite and the solvents were evaporated under reduced pressure. The crude product was purified *via* column chromatography with 5% ethyl acetate and hexane to afford the diarylated furanone product.

4.1.2.1. *5-(Diphenylmethylene)furan-2(5H)-one (6) [32].* Yield: 82%

^{1}H NMR ($CDCl_3$, 400 MHz): 6.21 (1H, d, *J* = 5.2 Hz, **H**-3), 7.26–7.50 (11H, m, **H**-4, **H**-2′, **H**-2″, **H**-3′, **H**-3″, **H**-4′, **H**-4″, **H**-5′, **H**-5″, **H**-6′, **H**-6″); ^{13}C NMR ($CDCl_3$, 100 MHz): 118.60 (**C**3), 128.24 and 128.49 (**C**2′, **C**6′, **C**2″, **C**6″), 128.75 (**C**6), 128.90 (**C**4′), 129.08 (**C**4″), 131.23 and 131.25 (**C**3′, **C**5′, **C**3″, **C**5″), 136.55 (**C**1′), 137.24 (**C**1″), 143.93 (**C**4), 147.13 (**C**5), 170.50 (**C**2); IR (ATR, cm^{-1}): 3056, 1768, 1746, 1545, 1491, 1444, 1230, 1110, 1069, 1031, 999, 931, 877, 772, 757, 695, 659; HRMS (ESI^+): Exact mass calculated for $C_{17}H_{13}O_2^+$ $[M+H]^+$ = 249.0916; Found = 249.0910.

4.1.2.2. 5-(Bis(2-methoxyphenyl)methylene)furan-2(5H)-one (8). Yield: 7%

^{1}H NMR ($CDCl_3$, 400 MHz): 3.65 (3H, s, OC**H$_3$'**), 3.74 (3H, s, OC**H$_3$**″), 6.15 (1H, d, *J* = 5.8 Hz, **H**-3), 6.89–6.98 (4H, m, **H**-5′, **H**-5″, **H**-3′, **H**-3″), 7.19 (2H, td, *J* = 8.3 Hz, 1.56 Hz, **H**-4′, **H**-4″), 7.26–7.35 (2H, m, **H**-6′, **H**-6″), 7.37 (1H, d, *J* = 5.8 Hz, **H**-4); ^{13}C NMR ($CDCl_3$, 100 MHz): 55.74 (O**C**H_3'), 55.86 (O**C**H_3″), 111.55 and 111.62 (**C**3′, **C**3″), 118.98 (**C**3), 120.21 and 120.30 (**C**5′, **C**5″), 122.73 and 126.31 (**C**1′, **C**1″), 126.50 (**C**6), 129.79 and 130.01 (**C**6′, **C**6″), 131.06 and 132.38 (**C**4′, **C**4″), 143.12 (**C**4), 148.09 (**C**5), 157.20 and 157.75 (**C**2′ and **C**2″), 170.51 (**C**2); IR (ATR, cm^{-1}): 3069, 3000, 2935, 2836, 1771, 1744, 1595, 1488, 1246, 1228, 1179, 1162, 1111, 1023, 961, 937, 881, 751; HRMS (ESI^+): Exact mass calculated for $C_{19}H_{17}O_4^+$ $[M+H]^+$ = 309.1127; Found = 309.1117.

4.1.2.3. 5-(Bis(3-methoxyphenyl)methylene)furan-2(5H)-one (10). Yield: 75%

^{1}H NMR ($CDCl_3$, 400 MHz): 3.79 (3H, s, OC**H$_3$**'), 3.80 (3H, s, OC**H$_3$**″), 6.20 (1H, d, *J* = 5.5 Hz, **H**-3), 6.80 (1H, dd, *J* = 2.4 Hz, 1.67 Hz, **H**-2′), 6.86–6.91 (2H, m, **H**-4′, **H**-6′), 6.96 (1H, ddd, *J* = 8.5 Hz, 2.7 Hz, 1.0 Hz, **H**-4″), 7.05–7.11 (2H, m, **H**-2″, **H**-6″), 7.26–7.35 (2H, m, **H**-5′, **H**-5″), 7.43 (1H, d, *J* = 5.5 Hz, **H**-4); ^{13}C NMR ($CDCl_3$, 100 MHz): 55.33 (O**C**H_3'), 55.36 (O**C**H_3″), 114.32 (**C**4″), 114.71 (**C**4′), 116.73 (**C**2″), 116.82 (**C**2′), 118.63 (**C**3), 123.68 (**C**6′), 123.82 (**C**6″), 128.22 (**C**6), 129.15 (**C**5′), 129.45 (**C**5″), 137.61 (**C**1′), 138.41 (**C**1″), 143.99 (**C**4), 147.22 (**C**5), 159.28 (**C**3′), 159.49 (**C**3″), 170.37 (**C**2); IR (ATR, cm^{-1}): 2959, 2935, 2835, 1779, 1750, 1594, 1574, 1486, 1429, 1286, 1247, 1207, 1109, 1047, 983, 889, 809, 792, 771, 736,; HRMS (ESI^+): Exact mass calculated for $C_{19}H_{17}O_4^+$ $[M+H]^+$ = 309.1127; Found = 309.1129.

4.1.2.4. 5-(Bis(4-methoxyphenyl)methylene)furan-2(5H)-one (12). Yield: 83%

^{1}H NMR ($CDCl_3$, 400 MHz): 3.84 (3H, s, OC**H$_3$**'), 3.87 (3H, s, OC**H$_3$**″), 6.14 (1H, d, *J* = 5.3 Hz, **H**-3), 6.88 (2H, d, *J* = 8.9 Hz, **H**-3″, **H**-5″), 6.94 (2H, d, *J* = 8.7 Hz, **H**-3′, **H**-5′), 7.19 (2H, d, *J* = 8.7 Hz, **H**-2′, **H**-6′), 7.40 (1H, d, *J* = 5.4 Hz, **H**-4), 7.47 (2H,d, *J* = 9.0 Hz, **H**-2″, **H**-6″); ^{13}C NMR ($CDCl_3$, 100 MHz): 55.37 (O**C**H_3'), 55.41 (O**C**$H_{3''}$), 113.68 (**C**3″, **C**5″), 113.86 (**C**3′, **C**5′), 117.13 (**C**3), 128.72 (**C**6), 129.27 (**C**1″), 129.61 (**C**1′), 132.60 (**C**2′, **C**6′), 133.06 (**C**2″, **C**6″), 143.93 (**C**4), 146.07 (**C**5), 160.21 (**C**4′), 160.28 (**C**4″), 170.98 (**C**2); IR (ATR, cm^{-1}): 3004, 2956, 2838, 1770, 1744, 1602, 1540, 1509, 1251, 1175, 1031, 883, 835, 562; HRMS (ESI^+): Exact mass calculated for $C_{19}H_{17}O_4^+$ $[M+H]^+$ = 309.1127; Found = 309.1118.

4.1.2.5. 5-(Bis(4-fluorophenyl)methylene)furan-2(5H)-one (14). Yield: 86%

^{1}H NMR ($CDCl_3$, 400 MHz): 6.23 (1H, d, *J* = 5.5 Hz, **H**-3), 7.06 (2H, t, *J* = 8.7 Hz, **H**-3″, **H**-5″), 7.14 (2H, t, *J* = 8.8 Hz, **H**-3′, **H**-5′), 7.23–7.26 (2H, m, **H**-2′, **H**-6′), 7.38 (1H, d, *J* = 5.5 Hz, **H**-4), 7.46–7.50 (2H, m, **H**-2″, **H**-6″); ^{13}C NMR ($CDCl_3$, 100 MHz): 115.47 (d, *J* = 21.7 Hz, **C**3″, **C**5″), 115.81 (d, *J* = 21.9 Hz, **C**3′, **C**5′), 118.88 (**C**3), 126.36 (**C**6), 132.48 (d, *J* = 3.47 Hz, **C**1′), 132.98 (d, *J* = 3.3 Hz, **C**1″), 132.8 (d, *J* = 8.3 Hz, **C**2′, **C**6′), 133.18 (d, *J* = 8.5 Hz, **C**2″, **C**6″), 143.54 (**C**4), 146.97 (**C**5), 162.99 (d, *J* = 251.0, **C**4′), 163.15 (d, *J* = 250.0 Hz, **C**4″), 170.21 (**C**2);

IR (ATR, cm^{-1}): 2923, 1770, 1746, 1596, 1546, 1504, 1343, 1233, 1158, 1107, 951, 879, 838, 807, 801, 570, 592, 524; HRMS (ESI^+): Exact mass calculated for $C_{17}H_{11}F_2O_2^+$ $[M+H]^+$ = 285.0721; Found = 285.0722.

4.1.2.6. 5-(Bis(4-(trifluoromethyl)phenyl)methylene)furan-2(5H)-one (16). Yield: 84%

^1H NMR ($CDCl_3$, 400 MHz): 6.34 (1H, d, J = 5.50 Hz, **H**-3), 7.41–7.43 (3H, m, **H**-4, **H**-2′, **H**-6′), 7.57 (2H, d, J = 8.5 Hz, **H**-2″, **H**-6″), 7.63 (2H, d, J = 8.51 Hz, **H**-3″, **H**-5″), 7.73 (2H, d, J = 8.1 Hz, **H**-3′, **H**-5′); ^{13}C NMR ($CDCl_3$, 75.5 MHz): 120.56 (**C**3), 122.53 (**C**6), 123.77 (q, J = 272.2 Hz, **C**F_3″), 123.80 (q, J = 272.2 Hz, **C**F_3'), 125.33 (q, J = 3.6 Hz, **C**3″, **C**5″), 125.76 (q, J = 3.6 Hz, **C**3′, **C**5′) 130.86 (q, J = 32.7 Hz, **C**4″), 131.32 (q, J = 32.7 Hz, **C**4′), 131.24 (**C**2″, **C**6″), 131.49 (**C**2′, **C**6′), 139.35 (**C**1″), 140.20 (**C**1), 143.11 (**C**4), 148.39 (**C**5), 169.36 (**C**2); IR (ATR, cm^{-1}): 3144, 1776, 1752, 1616, 1573, 1320, 1235, 1165, 1110, 1067, 1017, 966, 957, 923, 877, 769, 752, 731; HRMS (ESI^+): Exact mass calculated for $C_{19}H_{11}F_6O_2^+$ $[M+H]^+$ = 385.0663; Found = 385.0656.

4.1.2.7. 5-(Bis(3-nitrophenyl)methylene)furan-2(5H)-one (18). Yield: 11%

^1H NMR ($CDCl_3$, 300 MHz): 6.42 (1H, d, J = 5.6 Hz, **H**-3), 7.44 (1H, d, J = 5.6 Hz, **H**-4), 7.61–7.66 (2H, m, **H**-5″, **H**-6′), 7.72 (1H, t, J = 8.0 Hz, **H**-5′), 7.89 (1H, ddd, J = 7.9 Hz, 1.7 Hz, 1.1 Hz, **H**-6″), 8.17–8.20 (2H, m, **H**-2′, **H**-2″), 8.24 (1H, ddd, J = 8.2 Hz, 2.3 Hz, 1.1 Hz, **H**-4″), 8.36 (1H, ddd, J = 8.0 Hz, 2.3 Hz, 1.2 Hz, **H**-4′); ^{13}C NMR ($CDCl_3$, 75.5 MHz): 121.83 (**C**3), 122.97 (**C**6), 124.27 (**C**4″), 124.60 (**C**4′), 125.62 (**C**2″), 125.95 (**C**2′), 130.00 (**C**5″), 130.55 (**C**5′), 136.88 (**C**6″), 137.12 (**C**6′), 137.53 (**C**1″), 137.97 (**C**1′), 142.88 (**C**4), 148.63 (**C**3″), 148.84 (**C**3'), 149.58 (**C**5), 169.05 (**C**2); IR (ATR, cm^{-1}): 3082, 3924, 2854, 1781, 1754, 1526, 1345, 1235, 1201, 1075, 994, 879, 815, 762, 709, 662; HRMS (ESI^+): Exact mass calculated for $C_{17}H_{11}N_2O_6^+$ $[M+H]^+$ = 339.0617; Found = 339.0607.

4.1.2.8. 5-(Bis(4-nitrophenyl)methylene)furan-2(5H)-one (20). Yield: 8%

^1H NMR ($CDCl_3$, 300 MHz): 6.43 (1H, d, J = 5.5 Hz, **H**-3), 7.42 (1H, d, J = 5.5 Hz, **H**-4), 7.48 (2H, d, J = 8.5 Hz, **H**-2′, **H**-6′), 7.63 (2H, d, J = 8.7 Hz, **H**-2″, **H**-6″), 8.25 (2H, d, J = 8.7 Hz, **H**-3″, **H**-5″), 8.35 (2H, d, J = 8.5 Hz, **H**-3′, **H**-5′); ^{13}C NMR ($CDCl_3$, 75.5 MHz): 121.77 (**C**3), 123.05 (**C**6), 123.70 (**C**3″, **C**5″), 124.18 (**C**3′, **C**5′), 131.73 (**C**2″, **C**6″), 132.06 (**C**2′, **C**6′), 141.67 (**C**1′, **C**1″), 142.63 (**C**4), 147.67 (**C**4′), 148.31 (**C**4″), 149.21 (**C**5), 168.63 (**C**2); IR (ATR, cm^{-1}): 3109, 3077, 1778, 1754, 1552, 1515, 1406, 1344, 1191, 1107, 1041, 857, 845, 752, 734, 625; HRMS (ESI^+): Exact mass calculated for $C_{17}H_{11}N_2O_6^+$ $[M+H]^+$ = 339.0617; Found = 339.0606.

4.1.2.9. *5-(Di(thiophen-2-yl)methylene)furan-2(5H)-one (22) [32].* Yield: 25%

^1H NMR ($CDCl_3$, 300 MHz): 6.19 (1H, d, J = 5.7 Hz, **H**-3), 7.08 (1H, dd, J = 5.2 Hz, 3.9 Hz, **H**-4″), 7.13 (1H, dd, J = 5.2 Hz, 3.5 Hz, **H**-4′), 7.21 (1H, dd, J = 3.5 Hz, 1.3 Hz, **H**-3′), 7.42 (1H, dd, J = 3.9 Hz, 1.3 Hz, **H**-3″), 7.49 (1H, d, J = 5.7 Hz, **H**-4), 7.51 (1H, dd, J = 5.2 Hz, 1.3 Hz, **H**-5′), 7.55 (1H, dd, J = 5.2 Hz, 1.3 Hz, **H**-5″); ^{13}C NMR ($CDCl_3$, 75.5 MHz): 115.01 (**C**6), 118.11 (**C**3), 127.03 (**C**4′), 127.50 (**C**4″), 128.08 (**C**3″), 130.79 (**C**3′), 131.00 (**C**5″), 132.08 (**C**5′), 136.31 (**C**2′), 139.55 (**C**2″), 143.04 (**C**4), 146.23 (**C**5), 169.55 (**C**2); IR (ATR, cm^{-1}): 3106, 2921, 1780, 1761, 1579, 1539, 1412, 1238, 1105, 1066, 892, 806, 706; HRMS (ESI^+): Exact mass calculated for $C_{13}H_9O_2S_2^+$ $[M+H]^+$ = 261.0044; Found = 261.0036.

4.1.3. Synthesis of 5-(Bis(4-hydroxyphenyl)methylene)furan-2(5H)-one (21)

To an oven dried microwave reaction vial was added **3** (200 mg, 0.787 mmol), 4-hydroxyphenylboronic acid (326 mg, 2.363 mmol), sodium carbonate (251 mg, 2.368 mmol), bis(triphenylphosphine) palladium(II) dichloride (44 mg, 0.062 mmol), DME (2 mL) and ethanol (0.5 mL). The vial was flushed with nitrogen and heated at 120 °C in a microwave reactor for 40 min. The crude reaction mixture was filtered over a layer of Celite and the solvent was evaporated under reduced pressure. The crude product was purified *via* column chromatography with 10%–20% ethyl acetate in hexane to afford **21**.

Yield: 58%

^1H NMR ($CDCl_3$, 300 MHz): 6.09 (1H, d, J = 5.4 Hz, **H**-3), 6.84 (2H, d, J = 8.7 Hz, **H**-3″, **H**-5″), 6.89 (2H, d, J = 8.5 Hz, **H**-3′, **H**-5′), 7.09 (2H, d, J = 8.5 Hz, **H**-2′, **H**-6′), 7.38–7.41 (3H, m, **H**-4, **H**-2″, **H**-6″); ^{13}C NMR (DMSO-d_6), 75.5 MHz): 115.62 (**C**3″, **C**5″),115.81 (**C**3′, **C**5′), 117.19 (**C**6), 127.91 (**C**3), 128.07 (**C**1″), 129.23 (**C**1′), 132.92 (**C**2′, **C**6′), 133.18 (**C**2″, **C**6″), 144.85 (**C**4), 145.52 (**C**5), 158.73 (**C**4″), 158.87 (**C**4'), 170.80 (**C**2); IR (ATR, cm^{-1}): 3210, 2924, 2853, 1774, 1742, 1605, 1536, 1512, 1275, 1234, 1171, 1046, 1024, 954, 842, 810; HRMS (ESI^+): Exact mass calculated for $C_{17}H_{13}O_4^+$ $[M+H]^+$ = 281.0814; Found = 281.0808.

4.1.4. Synthesis of 5-(Dibromomethylene)-4-methylfuran-2(5H)-one (24) [29]

To a solution of methylsuccinic anhydride (1.606 mL, 17.844 mmol) in dichloromethane (40 mL) was slowly added a solution of carbon tetrabromide (8.876 g, 26.766 mmol) in dichloromethane (20 mL). The reaction mixture was cooled to 0 °C and triisopropylphosphite (8.804 mL, 35.684 mmol) in dichloromethane (10 mL) was added over 1 h. The mixture was stirred at room temperature for 2 h under nitrogen. The reaction was quenched with sodium bicarbonate (30 mL) and the mixture extracted with dichloromethane (3 x 30 mL). The combined organic layers were washed with brine (20 mL), dried with magnesium sulfate and the solvent was removed *in vacuo*. The crude product was purified by column chromatography with 2%–5% ethyl acetate in hexane to afford **24**.

Yield: 46%

H NMR ($CDCl_3$, 400 MHz): 2.48 (3H, d, J = 1.4 Hz, C**H**$_3$), 6.20 (1H, q, J = 1.4 Hz, **H**-3); ^{13}C NMR ($CDCl_3$, 100 MHz): 17.04 (**C**H_3), 80.68 (**C**Br_2), 121.04 (**C**3), 150.08 (**C**5), 153.87 (**C**4), 165.87 (**C**2); IR (ATR, cm^{-1}): 3114, 2922, 1770, 1759, 1603, 1383, 1325, 1254, 1235, 1056, 1033, 949, 905, 848, 820, 711, 651; HRMS (ESI^+): Exact mass calculated for $C_6H_5Br_2O_2^+$ $[M+H]^+$ = 266.8656; Found = 266.8648.

4.1.5. Synthesis of 4-(Bromomethyl)-5-(dibromomethylene)furan-2(5H)-one (27)

To a solution of 3-(bromomethyl)furan-2,5-dione (100 mg, 0.523 mmol) in dichloromethane (2 mL) was slowly added a solution of carbon tetrabromide (277 mg, 0.835 mmol) in dichloromethane (1 mL). The reaction mixture was cooled to 0 °C and triisopropylphosphite (0.258 mL, 1.047 mmol) in dichloromethane (0.5 mL) was added over 2 h. The mixture was stirred at room temperature for 4 h under nitrogen. The reaction was quenched with sodium bicarbonate and the mixture extracted with dichloromethane (3 x 10 mL). The combined organic layers were washed with brine, dried with magnesium sulfate and the solvent was removed *in vacuo*. The crude product was purified by careful column chromatography with 2%–10% ethyl acetate in hexane to furnish **27**.

Yield: 36%

^1H NMR ($CDCl_3$, 400 MHz): 4.57 (2H, d, J = 1.3 Hz, C**H**$_2$Br), 6.58 (1H, t, J = 1.3 Hz, **H**-3); ^{13}C NMR ($CDCl_3$, 100 MHz): 23.60 (**C**H_2Br), 81.45 (**C**6), 123.59 (**C**3), 147.64 (**C**5), 152.18 (**C**4), 164.36 (**C**2); IR (ATR, cm^{-1}): 3117, 2926, 1762, 1730, 1600, 1404, 1367, 1313, 1205, 1165, 1065, 1044, 956, 898, 864, 852, 832, 754, 736, 720, 679, 636, 536, 426; HRMS (ESI^+): Exact mass calculated for $C_6H_4Br_3O_2^+$ $[M+H]^+$ = 344.7761; Found 344.7766.

4.1.6. General ring-bromination procedure

To a stirred solution of the appropriate diarylated furanone (0.253

mmol, 1 eq.) in diethyl ether (0.4 mL) was slowly added a solution of bromine (0.01 mL, 0.251 mmol, 1 eq.) in diethyl ether or chloroform (0.4 mL). The reaction mixture was heated to reflux for 4 h, after which time the mixture was sparged with nitrogen for 10 min to remove excess bromine. The resulting solution was then cooled to 0 °C and a solution of triethylamine (0.07 mL, 0.503 mmol, 2 eq.) in diethyl ether (0.2 mL) was added dropwise over 10 min. The reaction was stirred for an additional hour at 0 °C before the reaction was allowed to reach room temperature. The reaction mixture was washed with water (3 x 5 mL) and brine (5 mL), dried over anhydrous magnesium sulfate and solvents were removed under reduced pressure. The crude reaction mixture was purified *via* column chromatography with 5%–10% ethyl acetate in hexane to afford the ring-brominated product.

4.1.6.1. 3-Bromo-5-(diphenylmethylene)furan-2(5H)-one (29). Yield: 81%

^{1}H NMR ($CDCl_3$, 300 MHz): 7.26–7.47 (10H, m, **H**-2′, **H**-2″, **H**-3′, **H**-3″, **H**-4′, **H**-4″, **H**-5′, **H**-5″, **H**-6′, **H**-6″), 7.52 (1H, s, **H**-4); ^{13}C NMR ($CDCl_3$, 75.5 MHz): 111.80 (**C**6), 128.35 and 128.65 (**C**2′, **C**6′, **C**2″, **C**6″), 129.25 and 129.45 (**C**4′, **C**4″), 129.69 (**C**5), 131.13 and 131.29 (**C**3′, **C**5′, **C**3″, **C**5″), 136.05 and 136.90 (**C**1′, **C**1″), 141.87 (**C**4), 145.38 (**C**5), 165.97 (**C**2); IR (ATR, cm^{-1}): 3057, 1761, 1545, 1492, 1444, 1228, 1109, 980, 924, 772, 741, 696, 659, 640; HRMS (ESI^+): Exact mass calculated for $C_{14}H_{12}BrO_2^+$ $[M+H]^+ = 327.0021$; Found = 327.0009.

4.1.6.2. 5-(Bis(4-methoxyphenyl)methylene)-3-bromofuran-2(5H)-one (30). Yield: 36%

^{1}H NMR ($CDCl_3$, 400 MHz): 3.84 (3H, s, OC**H**$_3$″), 3.88 (3H, s, OC**H**$_3$’), 6.89 (2H, d, $J = 8.7$ Hz, **H**-3″, **H**-5″), 6.95 (2H, d, $J = 8.5$ Hz, **H**-3′, **H**-5′), 7.19 (2H, d, $J = 8.5$ Hz, **H**-2′, **H**-6′), 7.44 (2H, d, $J = 8.7$ Hz, **H**-2″, **H**-6″), 7.49 (1H, s, **H**-4); ^{13}C NMR ($CDCl_3$, 75.5 MHz): 55.40 (OC**H**$_3$″), 55.45 (OC**H**$_3$’), 109.89 (**C**6), 113.81 (**C**3″, **C**5″), 114.03 (**C**3′, **C**5′), 128.74 (**C**3), 129.23 (**C**1′), 129.73 (**C**1″), 132.56 (**C**2′, **C**6′), 133.18 (**C**2″, **C**6″), 141.98 (**C**4), 144.28 (**C**5), 160.49 (**C**4′), 160.59 (**C**4″), 166.36 (**C**2); IR (ATR, cm^{-1}): 2917, 2848, 1768, 1594, 1496, 1287, 1266, 1054, 1016, 988, 816, 747, 668; HRMS (ESI^+): Exact mass calculated for $C_{19}H_{16}BrO_4^+$ $[M+H]^+ = 387.0232$; Found = 387.0231.

4.1.6.3. 5-(Bis(3-bromo-4-methoxyphenyl)methylene)-3-bromofuran-2(5H)-one (31). Yield: 34%

^{1}H NMR ($CDCl_3$, 400 MHz): 3.94 (3H, s, OC**H**$_3$″), 3.98 (3H, s, OC**H**$_3$’), 6.91 (1H, d, $J = 8.7$ Hz, **H**-5″), 6.97 (1H, d, $J = 8.4$ Hz, **H**-5′), 7.18 (1H, dd, $J = 8.4$ Hz, 2.18 Hz, **H**-6′), 7.44 (1H, d, $J = 2.2$ Hz, **H**-2′), 7.47 (1H, s, **H**-4), 7.48 (1H, dd, $J = 8.7$ Hz, 2.2 Hz, **H**-6″), 7.57 (1H, d, $J = 2.2$ Hz, **H**-2″); ^{13}C NMR ($CDCl_3$, 100 MHz): 56.40 (OC**H**$_3$″), 56.45 (OC**H**$_3$’), 111.47 (**C**5″), 111.62 (**C**6), 111.78 (**C**5′), 111.84 (**C**3″), 112.17 (**C**3′), 126.17 (**C**3), 129.59 (**C**1″), 129.94 (**C**1), 131.39 (**C**6′), 132.97 (**C**6″), 135.52 (**C**2′), 135.76 (**C**2″), 141.32 (**C**4), 145.10 (**C**5), 156.81 (**C**4′), 156.88 (**C**4″), 165.67 (**C**2); IR (ATR, cm^{-1}): 2917, 2848, 1768, 1594, 1496, 1461, 1439, 1287, 1266, 1054, 1016, 988, 816, 747, 668, 623; HRMS (ESI^+): Exact mass calculated for $C_{19}H_{14}Br_3O_4^+$ $[M+H]^+ = 542.8436$; Found = 542.8435.

4.1.6.4. 5-(Bis(4-(trifluoromethyl)phenyl)methylene)-3-bromofuran-2(5H)-one (32). Yield: 76%

^{1}H NMR ($CDCl_3$, 400 MHz): 7.42 (2H, d, $J = 8.1$ Hz, **H**-2′, **H**-6′), 7.51 (1H, s, **H**-4), 7.55 (2H, d, $J = 8.3$ Hz, **H**-2″, **H**-6″), 7.64 (2H, d, $J = 8.3$ Hz, **H**-3″, **H**-5″), 7.74 (2H, d, $J = 8.1$ Hz, **H**-3′, **H**-5′); ^{13}C NMR ($CDCl_3$, 100 MHz): 114.38 (**C**6) 123.68 (q, $J = 272.0$ Hz, **C**F_3’), 123.79 (q, $J = 271.7$ Hz, **C**F_3″), 125.47 (q, $J = 3.7$ Hz, **C**3″, **C**5″), 125.64 (**C**3), 125.95 (q, $J = 3.6$ Hz, **C**3′, **C**5′), 131.03 (q, $J = 32.62$ Hz, **C**4′), 131.26 (**C**2″, **C**6″), 131.37 (**C**2′, **C**6′), 131.61 (q, $J = 33.0$ Hz, **C**4″), 138.86 (**C**1′), 139.87 (**C**1″), 140.87 (**C**4), 146.73 (**C**5), 164.96 (**C**2); IR (ATR, cm^{-1}): 2923, 1852, 1772, 1617, 1552, 1410, 1321, 1235, 1160, 1130, 1117, 1109, 1069, 986, 855, 845, 730, 665, 610; HRMS (ESI^+): Exact mass calculated for $C_{19}H_{10}BrF_6O_2^+$ $[M+H]^+ = 462.9768$; Found = 462.9758.

4.1.7. Synthesis of (Z)-5-(chloroiodomethylene)furan-2(5H)-one (34) [29]

gem-Dichlorofuranone **33** (50 mg, 0.303 mmol), sodium iodide (454 mg, 3.030 mmol) and anhydrous DMF (1.8 mL) were placed in an oven-dried microwave reaction vial, flushed with nitrogen and sealed. The reaction mixture was heated to 160 °C for 3 min in a microwave reactor. The reaction mixture was then cooled to room temperature, poured onto ice water and extracted into diethyl ether (3 x 15 mL). The combined organic extracts were washed with water (15 mL) and brine (15 mL), dried over magnesium sulfate and the solvent was evaporated under reduced pressure. Purification of the crude reaction mixture *via* column chromatography with 4% ethyl acetate in hexane afforded **34**.

Yield: 43%

^{1}H NMR ($CDCl_3$, 400 MHz): 6.43 (1H, d, $J = 5.5$ Hz, **H**-3), 7.75 (1H, d, $J = 5.5$ Hz, **H**-4); ^{13}C NMR ($CDCl_3$, 100 MHz): 63.28 (**C**ICl), 122.28 (**C**3), 137.86 (**C**4), 154.15 (**C**5), 167.42 (**C**═O); IR (ATR, cm^{-1}): 3129, 3103, 3063, 1750, 1737, 1633, 1546, 1337, 1248, 1217, 1124, 1079, 971, 889, 844, 812, 711, 538; HRMS (ESI^+): Exact mass calculated for $C_5H_3ClIO_2^+$ $[M+H]^+ = 256.8866$; Found = 256.8856.

4.1.7.1. (Z)-5-(Chloro(phenyl)methylene)furan-2(5H)-one (35) [29]. Prepared using the general procedure for monoarylated furanones from *gem*-dichlorofuranone **33**.

Yield: 50%

^{1}H NMR ($CDCl_3$, 300 MHz): 6.28 (1H, d, $J = 5.5$ Hz, **H**-3), 7.47–7.51 (6H, m, **H**-4, **H**-2′, **H**-3′, **H**-4′, **H**-5′, **H**-6′); ^{13}C NMR ($CDCl_3$, 100 MHz): 120.42 (**C**3), 120.48 (**C**Cl), 128.85 and 129.60 (**C**2′, **C**6′, **C**3′, **C**5′), 130.43 (**C**4′), 134.00 (**C**1’), 141.44 (**C**4), 147.32 (**C**5), 168.46 (**C**2); IR (ATR, cm^{-1}): 3112, 3064, 1769, 1742, 1627, 1547, 1445, 1230, 1108, 1072, 961, 939, 869, 809, 759, 713, 695, 632, 543; HRMS (ESI^+) Exact mass calculated for $C_{11}H_8ClO_2^+$ $[M+H]^+ = 207.0213$; Found = 207.0207.

4.1.7.2. (Z)-5-(Chloro(4-methoxyphenyl)methylene)furan-2(5H)-one (36). Prepared using the general procedure for monoarylated furanones from *gem*-dichlorofuranone **33**.

Yield: 76%

^{1}H NMR ($CDCl_3$, 300 MHz): 3.87 (3H, s, OC**H$_3$**), 6.25 (1H, d, $J = 5.6$ Hz, **H**-3), 6.96–6.98 (2H, m, **H**-3′, **H**-5′), 7.43–7.45 (2H, m, **H**-2′, **H**-6′), 7.50 (1H, d, $J = 5.6$ Hz, **H**-4); ^{13}C NMR ($CDCl_3$, 75.5 MHz): 55.51 (O**C**H$_3$), 114.28 (**C**3′, **C**5′), 119.84 (**C**3), 120.72 (**C**Cl), 126.27 (**C**1′), 131.09 (**C**2′, **C**6′), 141.37 (**C**5), 146.63 (**C**4), 161.37 (**C**4’), 168.59 (**C**2); IR (ATR, cm^{-1}): 3025, 2922, 2848, 1770, 1746, 1604, 1544, 1509, 1413, 1301, 1254, 1237, 1176, 1110, 1029, 959, 872, 836, 808, 699, 682, 548; HRMS (ESI^+) Exact mass calculated for $C_{12}H_{10}ClO_3^+$ $[M+H]^+ = 237.0318$; Found = 237.0312.

4.1.8. Synthesis of 5-(1,5-dis(4-methoxyphenyl)penta-1,4-diyn-3-ylidene)furan-2(5H)-one (37)

gem-Dibromofuranone **3** (300 mg, 1.181 mmol), triphenylphosphine (62 mg, 20 mol%), bis(triphenylphosphine)palladium(II) dichloride (83 mg, 10 mol%) and copper iodide (45 mg, 20 mol%) were added to an oven-dried RBF under a flow of nitrogen. Diisopropylamine (5 mL) and 4-ethynylanisole (0.33 mL, 2.599 mmol) were subsequently added to the reaction flask. The mixture was stirred at 80 °C for 24 h after which time the reaction was quenched with saturated aqueous ammonium chloride solution. The mixture was extracted with dichloromethane (3 x 30 mL) and the combined organic layers were washed with water (3 x 30 mL) and brine (3 x 30 mL), dried with anhydrous magnesium sulfate and concentrated under reduced pressure. The crude product was purified by column chromatography with 5%–10% ethyl acetate in hexane to afford **37**.

Yield: 34%

^{1}H NMR ($CDCl_3$, 400 MHz): 3.84–3.85 (6H, m, OC**H$_3$**', OC**H$_3$**''), 6.29 (1H, d, J = 5.3 Hz, **H**-3), 6.88–6.91 (4H, m, **H**-3', **H**-5', **H**-3'', **H**-5''), 7.49 (2H, d, J = 8.8 Hz, **H**-2', **H**-6'), 7.54 (2H, d, J = 8.9 Hz, **H**-2'', **H**-6''), 7.86 (1H, d, J = 5.3 Hz, **H**-4); ^{13}C NMR ($CDCl_3$, 100 MHz) 55.38 and 55.40 (O**C**H$_3$', O**C**H$_3$''), 81.95 (**C**6), 82.61 and 92.76 (**C'**≡C', **C'**'≡C''), 95.28 and 100.65 (C'≡**C'**, C'≡**C''**), 113.86 and 114.06 (**C**1', **C**1''), 114.14 and 144.22 (**C**3', **C**5', **C**3'', **C**5''), 119.80 (**C**3), 133.41 (**C**2', **C**6'), 133.82 (**C**2'', **C**6''), 140.32 (**C**4), 158.38 (**C**5), 160.50 and 160.65 (**C**4', **C**4''), 168.63 (**C**2); IR (ATR, cm^{-1}): 2936, 2841, 2187, 1774, 1748, 1603, 1509, 1411, 1291, 1250, 1173, 1119, 1105, 1031, 875, 831, 806, 740, 565; HRMS (ESI$^+$): Exact mass calculated for $NaC_{23}H_{16}O_4^+$ $[M+Na]^+$ = 379.0936; Found = 379.0946.

4.2. Biological evaluation

4.2.1. Microbial strains and growth conditions

Bacterial strains were obtained from our own collection. *S. enterica* sv. Typhimurium was grown in tryptic soy broth 20 times diluted (1/20 TSB). *S. aureus* Newman (ATCC 25904) was grown in TSB 0.5 × TSB supplemented with 1% glucose. *P. aeruginosa* strains PAO1 and PAR7244, *E. coli* ATCC 9637 and *S. maltophilia* K279a were grown in LB broth (10 g/L tryptone, 5 g/L yeast extract and 10 g/L NaCl). All cultures were incubated at 37 °C and maintained on LB agar plates. If not stated otherwise, *C. albicans* M2396 [*adh1::(P_ADH1-RFP CaSAT1)*] was grown aerobically with shaking (180 rpm) at either 30 °C or 37 °C in YPD media (10 g/L yeast extract, 20 g/L peptone and 20 g/L D-(+)-glucose) supplemented with 200 μg/mL nourseothricin.

4.2.2. Fluorescently labelled strains

The *P. aeruginosa* strain PAO1 was fluorescently labelled with enhanced yellow fluorescent protein (eYFP), using the mini-Tn*7* delivery plasmid pUC18T-mini-Tn*7*T-Gm-*eyfp* (Addgene #65031) essentially as described previously [60,61]. For the construction of *P. aeruginosa* PAO1:eYFP, the plasmid pUC18T-mini-Tn*7*T-Gm-*eyfp* was transferred to the *P. aeruginosa* PAO1 wild-type by four-parental mating, involving *E. coli* DH5α/pRK2013 [62–64] and *E. coli* SM10 λ*pir*/pUX-BF13 [63,65] as helper strains, *E. coli* DH5α/pUC18T-mini-Tn*7*T-Gm-*eyfp* as the donor, and *P. aeruginosa* PAO1 as the recipient strain. The strains were grown in LB media, containing kanamycin (30 μg/mL) for *E. coli* DH5α/pRK2013, 100 μg/mL of ampicillin for *E. coli* SM10 λ*pir*/pUX-BF13, and ampicillin (100 μg/mL) and gentamycin (15 μg/mL) for *E. coli* DH5α/pUC18T-mini-Tn*7*T-Gm-*eyfp*. All strains were grown aerobically with shaking (220 rpm) at 37 °C in LB media, except *E. coli* SM10 λ*pir*/pUX-BF13 was routinely cultured at 30 °C. After overnight growth, the cells from 1 mL of each *E. coli* culture and 330 μL of *P. aeruginosa* PAO1 were harvested by centrifugation. To prepare a mating mixture, the cell pellets of all strains were pooled in 1 mL of LB medium, sedimented by centrifugation, resuspended in 100 μL of super optimal broth (SOB) (5 g/L yeast extract, 20 g/L tryptone, 10 mM NaCl, 2.5 mM KCl, 20 mM $MgSO_4$) and then spotted onto an SOB agar plate as described elsewhere for triparental mating experiments [66]. Following overnight incubation of the SOB agar plate at 30 °C, the bacterial spot was scraped and resuspended in 1 mL of PBS by rigorous vortexing to interrupt mating pairs. The *P. aeruginosa* PAO1 transconjugants were selected at 37 °C on Vogel-Bonner minimal medium (VBBM) (3 g/L trisodium citrate, 2 g/L citric acid, 10 g/L K_2HPO_4, 3.5 g/L $NaNH_4HPO_4{\cdot}4H_2O$, 1 mM $MgSO_4$, 100 μM $CaCl_2$, pH 7.0) agar plates containing 30 μg/ml of gentamycin [61]. The chromosomal insertion of the mini-Tn*7* element downstream of the *glmS* gene for glutamine–-fructose-6-phosphate aminotransferase was verified by PCR, using the primer pairs PTn7R [61] and PAO1-glmS-Ctrl1 (GCTGAAGCTCAAGGAAATTTCC), and PTn7L [61] and PAO1-PA5548-Ctr (TTACCTGCGACGTTATCTGAAGC) to amplify the flanking mini-Tn*7* regions, respectively.

The RFP-expressing *C. albicans* strain M2396 expressing the red fluorescence protein (RFP) was generated by transforming the wild-type strain *C. albicans* SC5314 [67] with an RFP-cassette obtained from plasmid pADH1R1 [68]. A single copy of the *ADH1* gene was replaced by the RFP-cassette yielding the RFP-labelled strain. Positive transformants were selected on YPD agar plates containing 200 μg/mL nourseothricin. The RFP signal was detected using the red channel (excitation/emission 555/584 – FLUO-N3) of a Leica microscope (Leica DM5500 B). The correct genomic integration of the RFP-cassette was confirmed by PCR and Southern blot analyses (data not shown).

4.2.3. Intrinsic cell growth inhibition

To evaluate the growth inhibition potential of furanone compounds, a variant of the broth microdilution method was used. Bacterial strains were grown overnight in the appropriated medium and then subcultured to new cultures with 1:100 dilution. 100 μL of fresh log phase cultures, adjusted to a final concentration of 1 × 10^5 cfu/mL, were added per well to 96-well sterile microtiter plates containing 100 μL of furanone at 0.1 mM (from a stock solution at 10 mM dissolved in DMSO) to obtain a final concentration of 0.05 mM. Plates were incubated at 37 °C for 20 h and then the optical density, determined at 550 nm (OD_{550nm}), was measured using a multilabel microtitre plate reader (Victor 3, PerkinElmer LAS, Waltham, MA, USA). Before readout, plates were shaken for homogenization. DMSO alone was included as control at final concentration of 0.5%. Bacterial growth was expressed in percentage on the basis of growth in control wells. The screening was done at least three times. The average of OD_{550nm} values of each sample was used to calculate the percentage of inhibition.

To assess the growth of *C. albicans* M2396 in the presence of furanones at 50 μM each, a fresh overnight culture of the yeast grown aerobically (180 rpm) at 30 °C in YPD medium was diluted to an OD_{600} of 0.05, followed by transfer of 199 μL of the diluted cell suspension to each well of a Corning 96 flat bottom transparent polystyrol microplate containing 1 μl of the compound stock solution (10 mM in DMSO). Corresponding controls consisting of 199 μL of the diluted cell suspension and 1 μL of DMSO were used as a reference to calculate the average percentage of growth inhibition by each individual furanone from four independent experiments. The microplates were incubated in a humidified chamber at 30 °C with shaking (100 rpm) for 20 h, followed by measurement of the OD_{600} values of the cell suspensions using a NanoQuant Infinite 200 Microplate Reader (Tecan Group, Gröding, Austria).

4.2.4. Biofilm inhibition assay

For biofilm formation, the crystal violet method was used as previously described, with some modifications [69]. Briefly, 100 μl of fresh log phase bacteria at a final concentration of 1 × 10^5 cfu/mL, were added to 96-well non-treated flat-bottom sterile microtiter plates (Deltalab S.L., Spain) containing 100 μL of furanones at 0.1 mM (0.05 mM as a final concentration). Plates were incubated for 24 h at 37 °C. The OD_{620nm} was determined using the microtitre plate reader (Victor 3) to measure bacterial biomass. Supernatants were then aspirated and the plates were washed three times with distilled water. In order to fix the biofilm, plates were incubated at 65 °C for 15 min. The biofilm was stained by adding 200 μL of 0.1% crystal violet and the plates were incubated for 15 min at room temperature. The crystal violet was discarded and the plates were washed three times with distilled water. The plates were allowed to dry, incubating at 37 °C for at least 30 min. To dissolve the crystal violet, 250 μl of 30% acetic acid was added. The plates were incubated for 15 min at room temperature and 150 μL was transferred to a new plate and the OD_{550nm} was measured. At least three replicates per strain and condition were tested. Growth control wells containing bacteria in the corresponding medium and control wells containing only sterile medium were included.

Biofilm formation of *C. albicans* M2396 upon exposure to furanones at 50 μM each was investigated by sustained and developmental inhibition assays according to published protocols [70]. For the sustained inhibition assay, the furanones were present in both a 90-min adherence

step and a 24-h growth period, whereas the developmental inhibition assay consisted of a 90-min adherence step in absence and a 24-h biofilm formation period in presence of the compounds. All other steps were identical for both assays. The OD_{600} of a fresh overnight culture of *C. albicans* M2396 grown aerobically (180 rpm) at 30 °C in YPD medium was adjusted to a value of 0.5. For the sustained inhibition assay, 199 μL of the cell suspension was added to each well of a Corning 96 flat bottom transparent polystyrol microplate along with 1 μL of the compound stock solution (10 mM in DMSO), whereas the wells of the developmental inhibition assay contained instead 1 μL of DMSO. The microplates were then incubated without shaking at 37 °C for 90 min. The media were aspirated and the wells were washed with 200 μL of PBS. A total volume of 200 μL of YPD medium with the appropriate compound was added to the corresponding well, and after an incubation of the microplates in a humidified chamber at 37 °C with shaking (100 rpm) for another 24 h, the medium was aspirated from each well. Following a washing step of the biofilm with 200 μL of PBS, cell viability was examined with the colorimetric 2,3-bis-(2-methoxy-4-nitro-5-sulfophenyl)-2*H*-tetrazolium-5-carboxanilide (XTT) reduction assay as described [70]. The OD_{492} values obtained in quadruplicate for each condition were averaged and normalized to averaged OD_{492} values of control biofilms formed in YPD medium with 0.5% of DMSO in both the adherence step and the growth period.

4.2.5. Confocal laser-scanning microscopy of mono- and dual-species biofilms

Confocal laser-scanning microscopy (CLSM) was used to investigate the effect of selected furanones at 50 μM each on the formation of mono- and dual-species biofilms. To prepare the inoculum for biofilm formation, the cell numbers of exponentially growing cultures of *P. aeruginosa* PAO1:eYFP and *C. albicans* M2396 were adjusted to 6.67×10^5 cfu/mL in LB media. Each well of a μ-Slide 8-Well ibiTreat slide (ibidi GmbH, Gräfelfing, Germany) was then seeded with a total volume of 300 μL, containing 1×10^5 cfu of each microorganism and 1.5 μL of the compound stock solution (10 mM in DMSO). For mono-species biofilms, 150 μL of the diluted cell suspension was mixed with 150 μL of LB medium, whereas the inoculum for dual-species biofilm formation consisted of 150 μL of each microorganism with a cell number of 6.67×10^5 cfu/ml. The corresponding control biofilms were grown in LB media containing 0.5% of DMSO. After incubation of the μ-Slides at 37 °C without shaking in a humidified chamber for 24 h, the culture supernatants were aspirated and the wells were washed with 300 μL of PBS. The biofilms were then fixed in the dark with 300 μL of a 2% paraformaldehyde solution in PBS at room temperature for 20 min. Finally, the biofilms were washed with 300 μL of PBS and overlayed with 150 μL of VECTASHIELD Antifade Mounting Medium (Biozol GmbH, Eching, Germany).

CLSM of the biofilms was performed with a TCS SP5 inverse confocal laser-scanning microscope (Leica Microsystems, Mannheim, Germany) and analysed with LAS AF software (version 2.73). The microscope was equipped with a Leica 63x/NA 1.40 HCX Plan Apochromat CS oil immersion objective. RFP of *C. albicans* M2396 was excited with 561 nm laser light and fluorescence emission was detected between 566 and 600 nm, whereas eYFP of *P. aeruginosa* PAO1:eYFP was excited with 514 nm laser light and fluorescence emission was detected between 520 and 560 nm.

4.2.6. Cytotoxicity assay

To determinate the cytotoxic effect of furanones on HK-2 tubular cells, the kit CellTiter 96 Aqueous solution (Promega) was used following the manufacturer's instructions. HK-2 cells were seeded at a concentration of 3.5×10^3 cells per well in 96-well tissue culture plates with clear bottoms (Nunc™ MicroWell™ 96-Well, Nunclon Delta-Treated®), using DMEM/F-12 GlutaMAX™ (Gibco™) supplemented with 10% Fetal Bovine Serum and 1 × Insulin-Transferrin-Selenium (Gibco™). The plates were incubated for 24 h (37 °C in 5% CO_2 atmosphere). Furanones were diluted to 50 μM in 200 μl of DMEM per well and incubated for 24 and 48 h. The culture medium was then removed. Next, 100 μL of fresh medium and 20 μL of CellTiter 96 aqueous reagent were added to each well. The absorbance was read after 4 h of incubation. A microplate reader (PerkinElmer Victor 3) was used with a wavelength of 450 nm and 620 nm. The results are expressed as viability percentage using cells unexposed as a control.

4.2.7. In vivo efficacy in the Galleria mellonella infection model

The larval stage of greater wax moth *G. mellonella* was used to evaluate the effect of furanones following bacterial infection. Larvae were obtained from our own hatchery. At least 15 larvae with no signs of melanization and a weight of 300–400 mg were used to infect *P. aeruginosa* PAR7244. The inoculum was obtained from a log-phase culture in appropriate media. Log-phase cultures were washed and adjusted in PBS to the desired doses, based on pilot studies (data not shown). The infective dose for *P. aeruginosa* PAR7244 was $1.6–3.2 \times 10^2$ cfu per larva. The cell number of the inoculum was confirmed by viable counts on LB agar plates. Larvae were infected injecting 5 μL of bacteria in the last left proleg using a 50-μL Hamilton® Microliter™ syringe. Larvae were incubated at 30 °C for 60 min. After incubation, 5 μL of a PBS solution containing either DMSO (untreated group) or furanone at a final concentration of 50 μM was injected in the last right proleg. The amount of furanones or DMSO solution injected was obtained according to the larvae weight as was previously described [71]. Larvae were incubated at 30 °C in darkness and the survival was recorded every 24 h. Larvae were considered dead when they were unresponsive to touch and turned dark brown or black in colour. At least two replicates of the experiments were made with different batches of larvae. Kaplan-Meier survival curves were plotted using GraphPad Prism and statistical significance was determined using the log rank (Mantel Cox) test.

Declaration of competing interest

The authors declare that they have no known competing financial interests or personal relationships that could have appeared to influence the work reported in this paper.

Data availability

Data is available in the Supplementary Data.

Acknowledgements

TL was supported by the School of Pharmacy University College Cork and Future University Egypt with a PhD Scholarship. CGMG acknowledges support from Science Foundation Ireland in the form of a center grant (APC Microbiome Ireland grant SFI/12/RC/2273_P2). ACG, DY, MB, XD and IG acknowledge financial support from the Spanish Ministry for Science, Innovation and Universities (grant PID2019-111364RB-I00). UM and SB are grateful to the Leibniz Association for financial support (grant SAS-2021-1-FZB of the Leibniz Research Alliance *INFECTIONS in an Urbanizing World - Humans, Animals, Environments*). We thank Manuel Hein, Dörte Grella (RCB) for expert technical assistance and the Fluorescence Cytometry Core Facility of the RCB for continuous support. We thank Herbert P. Schweizer (Colorado State University, Fort Collins, USA) for the plasmid pUC18T-mini-Tn7T-Gm-eyfp (Addgene # 65031) and Holger Lößner (Paul-Ehrlich-Institute, Federal Institute for Vaccines and Biomedicines, Langen, Germany) for *E. coli* SM10 λ*pir*/pUX-BF13.

Appendix A. Supplementary data

Supplementary data to this article can be found online at https://doi.org/10.1016/j.ejmech.2022.114678.

Supplementary data

Supplementary data associated with this article can be found in the online version, at **XXXXX**.

References

[1] L. Zaffiri, J. Gardner, L.-H. Toledo-Pereyra, History of antibiotics. From Salvarsan to Cephalosporins, J. Invest. Surg. 25 (2012) 67–77, https://doi.org/10.3109/08941939.2012.664099.

[2] K.C. Nicolaou, S. Rigol, A brief history of antibiotics and select advances in their synthesis, J. Antibiot. 71 (2018) 153–184, https://doi.org/10.1038/ja.2017.62.

[3] E.B. Chain, Academic and industrial contributions to drug research, Nature 200 (1963) 441–451, https://doi.org/10.1038/200441a0.

[4] T.C. Porco, T. Gebre, B. Ayele, J. House, J. Keenan, Z. Zhou, K.C. Hong, N. Stoller, K.J. Ray, P. Emerson, B.D. Gaynor, T.M. Lietman, Effect of mass distribution of azithromycin for trachoma control on overall mortality in Ethiopian children: a randomized trial, JAMA 302 (2009) 962–968, https://doi.org/10.1001/jama.2009.1266.

[5] C.P. Miller, Development of bacterial resistance to antibiotics, JAMA 135 (1947) 749–751, https://doi.org/10.1001/jama.1947.02890120003002.

[6] O.B. Jonas, A. Irwin, F.C.J. Berthe, F.G. Le Gall, P.V. Marquez, Drug-resistant Infections : a Threat to Our Economic Future, The World Bank, 2017.

[7] J. O'Neill, Review on Antimicrobial Resistance, Antimicrobial Resistance - Tackling a Crisis for the Health and Wealth of Nations, 2014.

[8] Antimicrobial Resistance Collaborators, Global burden of bacterial antimicrobial resistance in 2019: a systematic analysis, Lancet 399 (2022) 629–655, https://doi.org/10.1016/s0140-6736(21)02724-0.

[9] S.J. Baker, D.J. Payne, R. Rappuoli, E. De Gregoriob, Technologies to address antimicrobial resistance, Proc. Natl. Acad. Sci. USA 115 (2018) 12887–12895, https://doi.org/10.1073/pnas.1717160115.

[10] M.E. Olson, H. Ceri, D.W. Morck, A.G. Buret, R.R. Read, Biofilm bacteria: formation and comparative susceptibility to antibiotics,, Can. J. Vet. Res. 66 (2002) 86–92. PMCID: PMC226988.

[11] D. Sharma, L. Misba, A.U. Khan, Antibiotics versus biofilm: an emerging battleground in microbial communities, Antimicrob. Resist. Infect. Control 8 (2019) 1–10, https://doi.org/10.1186/s13756-019-0533-3.

[12] I.S. Sharafutdinov, E.Y. Trizna, D.R. Baidamshina, M.N. Ryzhikova, R. R. Sibgatullina, A.M. Khabibrakhmanova, L.Z. Latypova, A.R. Kurbangalieva, E. V. Rozhina, M. Klinger-Strobel, R.F. Fakhrullin, M.W. Pletz, M.I. Bogachev, A. R. Kayumov, O. Makarewicz, Antimicrobial effects of sulfonyl derivative of 2(5*H*)-Furanone against planktonic and biofilm associated methicillin-resistant and -susceptible *Staphylococcus aureus*, Front. Microbiol. 8 (2017), https://doi.org/10.3389/fmicb.2017.02246.

[13] T. Grainha, P. Jorge, D. Alves, S.P. Lopes, M.O. Pereira, Unraveling *Pseudomonas aeruginosa* and *Candida albicans* communication in coinfection scenarios: insights through network analysis, Front. Cell. Infect. Microbiol. 10 (2020), https://doi.org/10.3389/fcimb.2020.550505.

[14] M.B. Miller, B.L. Bassler, Quorum sensing in bacteria, Annu. Rev. Microbiol. 55 (2001) 165–199, https://doi.org/10.1146/annurev.micro.55.1.165.

[15] B.L. Bassler, S. Mukherjee, Bacterial quorum sensing in complex and dynamically changing environments, Nat. Rev. Microbiol. 17 (2019) 371–382, https://doi.org/10.1038/s41579-019-0186-5.

[16] W.R.J.D. Galloway, J.T. Hodgkinson, S.D. Bowden, M. Welch, D.R. Spring, Quorum sensing in gram-negative bacteria: small-molecule modulation of AHL and AI-2 quorum sensing pathways, Chem. Rev. 111 (2011) 28–67, https://doi.org/10.1021/cr100109t.

[17] L. Zhou, Y. Zhang, Y. Ge, X. Zhu, J. Pan, Regulatory mechanisms and promising applications of quorum sensing-inhibiting agents in control of bacterial biofilm formation, Front. Microbiol. 11 (2020), https://doi.org/10.3389/fmicb.2020.589640.

[18] R. de Nys, A.D. Wright, G.M. König, O. Sticher, New halogenated furanones from the marine alga *delisea pulchra* (*cf. fimbriata*), Tetrahedron 49 (1993) 11213–11220, https://doi.org/10.1016/S0040-4020(01)81808-1.

[19] S. Kjelleberg, P. Steinberg, M. Givskov, L. Gram, M. Manefield, R. de Nys, Do marine natural products interfere with prokaryotic AHL regulatory systems? Aquat. Microb. Ecol. 13 (1997) 85–93, https://doi.org/10.3354/ame013085.

[20] J.C.A. Janssens, H. Steenackers, S. Robijns, E. Gellens, J. Levin, H. Zhao, K. Hermans, D. De Coster, T.L. Verhoeven, K. Marchal, J. Vanderleyden, D.E. De Vos, S.C.J. De Keersmaecker, Brominated furanones inhibit biofilm formation by *Salmonella enterica* Serovar Typhimurium,, Appl. Environ. Microbiol. 74 (2008) 6639–6648, https://doi.org/10.1128/AEM.01262-08.

[21] M. Hentzer, M. Givskov, Pharmacological inhibition of quorum sensing for the treatment of chronic bacterial infections, J. Clin. Investig. 112 (2003) 1300–1307, https://doi.org/10.1172/JCI200320074.

[22] Y. Han, S. Hou, K.A. Simon, D. Ren, Y.-Y. Luk, Identifying the important structural elements of brominated furanones for inhibiting biofilm formation by *Escherichia coli*,, Bioorg. Med. Chem. Lett. 18 (2008) 1006–1010, https://doi.org/10.1016/j.bmcl.2007.12.032.

[23] J. Lonn-Stensrud, M.A. Landin, T. Benneche, F.C. Petersen, A.A. Scheie, Furanones, potential agents for preventing *Staphylococcus epidermidis* biofilm infections? J. Antimicrob. Chemother. 63 (2009) 309–316, https://doi.org/10.1093/jac/dkn501.

[24] T. Lyons, C.G.M. Gahan, T.P. O'Sullivan, Structure–activity relationships of furanones, dihydropyrrolones and thiophenones as potential quorum sensing inhibitors, Future Med. Chem. 12 (2020) 1925–1943, https://doi.org/10.4155/fmc-2020-0244.

[25] C.S. Pereira, J.A. Thompson, K.B. Xavier, AI-2-mediated signalling in bacteria, FEMS Microbiol. Rev. 37 (2013) 156–181, https://doi.org/10.1111/j.1574-6976.2012.00345.x.

[26] T. Zang, B.W.K. Lee, L.M. Cannon, K.A. Ritter, S. Dai, D. Ren, T.K. Wood, Z.S. Zhou, A naturally occurring brominated furanone covalently modifies and inactivates LuxS, Bioorg. Med. Chem. Lett 19 (2009) 6200–6204, https://doi.org/10.1016/j.bmcl.2009.08.095.

[27] M. Manefield, R. de Nys, N. Kumar, R. Read, M. Givskov, P. Steinberg, S. Kjelleberg, Evidence that halogenated furanones from *Delisea pulchra* inhibit acylated homoserine lactone (AHL)-mediated gene expression by displacing the AHL signal from its receptor protein, Microbiol. 145 (Pt 2) (1999) 283–291, https://doi.org/10.1099/13500872-145-2-283.

[28] H. Wu, Z. Song, M. Hentzer, J.B. Andersen, S. Molin, M. Givskov, N. Hoiby, Synthetic furanones inhibit quorum-sensing and enhance bacterial clearance in *Pseudomonas aeruginosa* lung infection in mice, J. Antimicrob. Chemother. 53 (2004) 1054–1061, https://doi.org/10.1093/jac/dkh223.

[29] T. Lyons, C.G.M. Gahan, T.P. O'Sullivan, Synthesis and reactivity of dihalofuranones, Lett. Org. Chem. 19 (2022) 662–667, https://doi.org/10.2174/1570178618666211027103633.

[30] S. Couty, M. Barbazanges, C. Meyer, J. Cossy, Palladium-catalyzed Suzuki-Miyaura coupling reactions involving β,β-dihaloenamides: application to the synthesis of disubstituted Ynamides, Synlett 2005 (2005) 905–910, https://doi.org/10.1055/s-2005-864821.

[31] L. Jeanne-Julien, G. Masson, E. Astier, G. Genta-Jouve, V. Servajean, J.-M. Beau, S. Norsikian, E. Roulland, Study of the construction of the Tiacumicin B aglycone, J. Org. Chem. 83 (2018) 921–929, https://doi.org/10.1021/acs.joc.7b02909.

[32] E. Marchal, P. Uriac, Y. Brunel, S. Poigny, Methylene Furanone Derivatives and Use of Said Derivatives as a Photoprotecting or Antioxidant or Depigmentation Agent in Cosmetic or Dermatological Compositions, US Patent US8563548B2, 2013.

[33] D. Nöteberg, W. Schaal, E. Hamelink, L. Vrang, M. Larhed, High-speed optimization of inhibitors of the malarial proteases plasmepsin I and II, J. Comb. Chem. 5 (2003) 456–464, https://doi.org/10.1021/cc0301014.

[34] H.P. Steenackers, J. Levin, J.C. Janssens, A. De Weerdt, J. Balzarini, J. Vanderleyden, D.E. De Vos, S.C. De Keersmaecker, Structure-activity relationship of brominated 3-alkyl-5-methylene-2(5*H*)-furanones and alkylmaleic anhydrides as inhibitors of *Salmonella* biofilm formation and quorum sensing regulated bioluminescence in *Vibrio harveyi*, Bioorg. Med. Chem. 18 (2010) 5224–5233, https://doi.org/10.1016/j.bmc.2010.05.055.

[35] C. Reynaud, H. Doucet, M. Santelli, Synthesis of Spherical Polyols from Itaconic Acid, Synthesis 2010 (2010) 1787–1792, https://doi.org/10.1055/s-0029-1218764.

[36] N.N. Biswas, G.M. Iskander, M. Mielczarek, T.T. Yu, D.S. Black, N. Kumar, Alkyne-substituted fimbrolide analogues as novel bacterial quorum-sensing inhibitors, Aust. J. Chem. 71 (2018) 708–715, https://doi.org/10.1071/CH18194.

[37] R. Franzén, L. Kronberg, Synthetic approaches to chlorinated 5-hydroxy-5-methyl-2-furanones, Tetrahedron 49 (1993) 10945–10958, https://doi.org/10.1016/S0040-4020(01)80248-9.

[38] R. Franzén, L. Kronberg, Synthesis of chlorinated 5-hydroxy 4-methyl-2(5*H*)-furanones and mucochloric acid, Tetrahedron Lett. 36 (1995) 3905–3908, https://doi.org/10.1016/0040-4039(95)00638-S.

[39] S.M. Jajere, A review of *Salmonella enterica* with particular focus on the pathogenicity and virulence factors, host specificity and antimicrobial resistance including multidrug resistance, Vet. World 12 (2019) 504–521, https://doi.org/10.14202/vetworld.2019.504-521.

[40] K.M. Craft, J.M. Nguyen, L.J. Berg, S.D. Townsend, Methicillin-resistant *Staphylococcus aureus* (MRSA): antibiotic-resistance and the biofilm phenotype, Med. Chem. Comm. 10 (2019) 1231–1241, https://doi.org/10.1039/c9md00044e.

[41] C.B. Creech, D.N. Al-Zubeidi, S.A. Fritz, Prevention of recurrent staphylococcal skin infections, Infect. Dis. Clin. 29 (2015) 429–464, https://doi.org/10.1016/j.idc.2015.05.007.

[42] S.Y. Tong, J.S. Davis, E. Eichenberger, T.L. Holland, V.G. Fowler Jr., *Staphylococcus aureus* infections: epidemiology, pathophysiology, clinical manifestations, and management, Clin. Microbiol. Rev. 28 (2015) 603–661, https://doi.org/10.1128/cmr.00134-14.

[43] N. Allocati, M. Masulli, M.F. Alexeyev, C. Di Ilio, *Escherichia coli* in Europe: an overview, Int. J. Environ. Res. Publ. Health 10 (2013) 6235–6254, https://doi.org/10.3390/ijerph10126235.

[44] J.S. Brooke, *Stenotrophomonas maltophilia*: an emerging global opportunistic pathogen, Clin. Microbiol. Rev. 25 (2012) 2–41, https://doi.org/10.1128/cmr.00019-11.

[45] P. Huedo, X. Coves, X. Daura, I. Gibert, D. Yero, Quorum sensing signaling and quenching in the multidrug-resistant pathogen *Stenotrophomonas maltophilia*, Front. Cell. Infect. Microbiol. 8 (2018) 1–8, https://doi.org/10.3389/fcimb.2018.00122.

[46] A. Litwin, S. Rojek, W. Gozdzik, W. Duszynska, *Pseudomonas aeruginosa* device associated - healthcare associated infections and its multidrug resistance at intensive care unit of University Hospital: polish, 8.5-year, prospective, single-centre study, BMC Infect. Dis. 21 (2021) 1–8, https://doi.org/10.1186/s12879-021-05883-5.

[47] G.P. Bodey, R. Bolivar, V. Fainstein, L. Jadeja, Infections caused by *Pseudomonas aeruginosa*, Rev. Infect. Dis. 5 (1983) 279–313, https://doi.org/10.1093/clinids/5.2.279.

[48] M. Gomes-Fernandes, A.-C. Gomez, M. Bravo, P. Huedo, X. Coves, C. Prat-Aymerich, I. Gibert, A. Lacoma, D. Yero, Strain-specific interspecies interactions between co-isolated pairs of *Staphylococcus aureus* and *Pseudomonas aeruginosa* from patients with tracheobronchitis or bronchial colonization, Sci. Rep. 12 (2022) 1–15, https://doi.org/10.1038/s41598-022-07018-5.
[49] F.L. Mayer, D. Wilson, B. Hube, *Candida albicans* pathogenicity mechanisms, Virulence 4 (2013) 119–128, https://doi.org/10.4161/viru.22913.
[50] R. Pereira, R.O. Dos Santos Fontenelle, E.H.S. De Brito, S.M. De Morais, Biofilm of *Candida albicans*: formation, regulation and resistance, J. Appl. Microbiol. 131 (2020) 11–22, https://doi.org/10.1111/jam.14949.
[51] P. Uppuluri, J. Nett, J. Heitman, D. Andes, Synergistic effect of calcineurin inhibitors and fluconazole against *Candida albicans* biofilms, Antimicrob. Agents Chemother. 52 (2008) 1127–1132, https://doi.org/10.1128/aac.01397-07.
[52] M. Gulati, C.J. Nobile, *Candida albicans* biofilms: development, regulation, and molecular mechanisms, Microb. Infect. 18 (2016) 310–321, https://doi.org/10.1016/j.micinf.2016.01.002.
[53] M. Duo, M. Zhang, Y.-Y. Luk, D. Ren, Inhibition of *Candida albicans* growth by brominated furanones, Appl. Microbiol. Biotechnol. 85 (2010) 1551–1563, https://doi.org/10.1007/s00253-009-2174-6.
[54] M.E. Shirtliff, B.M. Peters, M.A. Jabra-Rizk, Cross-kingdom interactions: *Candida albicans* and bacteria, FEMS Microbiol. Lett. 299 (2009) 1–8, https://doi.org/10.1111/j.1574-6968.2009.01668.x.
[55] E. Allegra, R.W. Titball, J. Carter, O.L. Champion, *Galleria mellonella* larvae allow the discrimination of toxic and non-toxic chemicals, Chemosphere 198 (2018) 469–472, https://doi.org/10.1016/j.chemosphere.2018.01.175.
[56] L. Hill, N. Veli, P.J. Coote, Evaluation of *Galleria mellonella* larvae for measuring the efficacy and pharmacokinetics of antibiotic therapies against *Pseudomonas aeruginosa* infection, Int. J. Antimicrob. Agents 43 (2014) 254–261, https://doi.org/10.1016/j.ijantimicag.2013.11.001.
[57] WHO, Antimicrobial Resistance, Global Report on Surveillance, WHO Reports, World Health Organization, Geneva, Switzerland, 2014.
[58] A. Sorg, K. Siegel, R. Brukner, Stereoselective syntheses of dihydroxerulin and xerulinic acid, anti-hypocholesterolemic dyes from the fungus *Xerula melanotricha*, Chem. Eur J. 11 (2005) 1610–1624, https://doi.org/10.1002/chem.200400913.
[59] A.J. Manny, S. Kjelleberg, N. Kumar, R. de Nys, R.W. Read, P. Steinberg, Reinvestigation of the sulfuric acid-catalysed cyclisation of brominated 2-alkylle-vulinic acids to 3-alkyl-5-methylene-2(5H)-furanones, Tetrahedron 53 (1997) 15813–15826, https://doi.org/10.1016/S0040-4020(97)10034-5.
[60] K.-H. Choi, J.B. Gaynor, K.G. White, C. Lopez, C.M. Bosio, R.R. Karkhoff-Schweizer, H.P. Schweizer, A Tn*7*-based broad-range bacterial cloning and expression system, Nat. Methods 2 (2005) 443–448, https://doi.org/10.1038/nmeth765.
[61] K.-H. Choi, H.P. Schweizer, mini-Tn*7* insertion in bacteria with single attTn*7* sites: example *Pseudomonas aeruginosa*, Nat. Protoc. 1 (2006) 153–161, https://doi.org/10.1038/nprot.2006.24.
[62] D.H. Figurski, D.R. Helinski, Replication of an origin-containing derivative of plasmid RK2 dependent on a plasmid function provided in *trans*, Proc. Natl. Acad. Sci. USA 76 (1979) 1648–1652, https://doi.org/10.1073/pnas.76.4.1648.
[63] V.L. Miller, J.J. Mekalanos, A novel suicide vector and its use in construction of insertion mutations: osmoregulation of outer membrane proteins and virulence determinants in *Vibrio cholerae* requires toxR, J. Bacteriol. 170 (1988) 2575–2583, https://doi.org/10.1128/jb.170.6.2575-2583.1988.
[64] R. Simon, U. Priefer, A. Pühler, A broad host range mobilization system for *in vivo* genetic engineering: transposon mutagenesis in Gram negative bacteria, Biotechnology 1 (1983) 784–791, https://doi.org/10.1038/nbt1183-784.
[65] Y. Bao, D.P. Lies, H. Fu, G.P. Roberts, An improved Tn7-based system for the single-copy insertion of cloned genes into chromosomes of Gram-negative bacteria, Gene 109 (1991) 167–168, https://doi.org/10.1016/0378-1119(91)90604-a.
[66] D.F. Aubert, M.A. Hamad, M.A. Valvano, A markerless deletion method for genetic manipulation of *Burkholderia cenocepacia* and other multidrug-resistant gram-negative bacteria, in: A. Vergunst, D. O'Callaghan (Eds.), Host-Bacteria Interactions, Humana Press, New York, 2014, pp. 311–327.
[67] A.M. Gillum, E.Y. Tsay, D.R. Kirsch, Isolation of the *Candida albicans* gene for orotidine-5'-phosphate decarboxylase by complementation of *S. cerevisiae* ura3 and *E. coli* pyrF mutations, Mol. Gen. Genet. 198 (1984) 179–182, https://doi.org/10.1007/bf00328721.
[68] C. Sasse, N. Dunkel, T. Schäfer, S. Schneider, F. Dierolf, K. Ohlsen, J. Morschhäuser, The stepwise acquisition of fluconazole resistance mutations causes a gradual loss of fitness in *Candida albicans*, Mol. Microbiol. 86 (2012) 539–556, https://doi.org/10.1111/j.1365-2958.2012.08210.x.
[69] P. Huedo, D. Yero, S. Martínez-Servat, I. Estibariz, R. Planell, P. Martínez, A. Ruyra, N. Roher, I. Roca, J. Vila, X. Daura, I. Gibert, Two different *rpf* clusters distributed among a population of *Stenotrophomonas maltophilia* clinical strains display differential diffusible signal factor production and virulence regulation, J. Bacteriol. 196 (2014) 2431–2442, https://doi.org/10.1128/jb.01540-14.
[70] M. Gulati, M.B. Lohse, C.L. Ennis, R.E. Gonzalez, A.M. Perry, P. Bapat, A. V. Arevalo, D.L. Rodriguez, C.J. Nobile, *In vitro* culturing and screening of *Candida albicans* biofilms, Curr. Protoc. Microbiol. 50 (2018) e60, https://doi.org/10.1002/cpmc.60.
[71] A. Andrea, K.A. Krogfelt, H. Jenssen, Methods and challenges of using the greater wax moth (*Galleria mellonella*) as a model organism in antimicrobial compound discovery, Microorganisms 7 (2019) 1–9, https://doi.org/10.3390/microorganisms7030085.